Global Journal of Pure and Applied Mathematics.
ISSN 0973-1768 Volume 13, Number 7 (2017), pp. 3403-3432

http://www.ripublication.com

Effect of Viscous Dissipation on Slip Boundary Layer Flow of Non-Newtonian Fluid over a Flat Plate with Convective Thermal Boundary Condition

Shashidar Reddy Borra

Department of Mathematics and Humanities, Mahatma Gandhi Institute of Technology, Gandipet, R.R.District-500075, Telangana, India.

Abstract

The purpose of this paper is to investigate the magnetic effects of a steady, two dimensional boundary layer flow of an incompressible non-Newtonian power-law fluid over a flat plate with convective thermal and slip boundary conditions by considering the viscous dissipation. The resulting governing non-linear partial differential equations are transformed into non linear ordinary differential equations by using similarity transformation. The momentum equation is first linearized by using Quasi-linearization technique. The set of ordinary differential equations are solved numerically by using implicit finite difference scheme along with the Thomas algorithm. The solution is found to be dependent on six governing parameters including Knudsen number Kn_x, heat transfer parameter ϕ, magnetic field parameter M, power-law fluid index n, Eckert number E_c and Prandtl number P_r. The effects of these parameters on the velocity and temperature profiles are discussed. The special interest are the effects of the Knudsen number Kn_x, heat transfer parameter ϕ and Eckert number E_c on the skin friction $f''(0)$, temperature at the wall $\theta(0)$ and the rate of heat transfer $\theta'(0)$. The numerical results are tabulated for $f''(0), \theta(0)$ and $\theta'(0)$.

Keywords: Magnetic field parameter, Knudsen number, Heat transfer parameter, Prandtl number, Viscous Dissipation and Non-Newtonian fluid.

Mathematics subject Classification: 76-00

NOMENCLATURE :

B – Magnetic field intensity
f - Dimensionless stream function
g – Acceleration due to gravity
k – Coefficient of conductivity of the fluid
M – Magnetic field parameter
n – Power-law index
Q – Heat source coefficient
T- Temperature of the fluid
u, v – Velocity components along and perpendicular to the plate
x, y – Coordinates along and perpendicular to the plate

Greek symbols

α – Ratio of accommodation factor
β – Coefficient of thermal expansion
γ – Heat source parameter
η – Dimensionless similarity variable
μ – Magnetic permeability
μ_0 – Dynamic coefficient of viscosity
ν - Kinematic viscosity
θ – Dimensionless temperature
ϕ - Heat transfer coefficient
ρ – Density
σ – Electrical conductivity
σ^* - Stefan-Boltzmann constant
τ_w - Shearing stress on the surface

Subscripts and super scripts

c_p – Specific heat capacity
C_f – Skin friction coefficient
E_c –Eckert number
F_M – Momentum accommodation factor
G_r – Grashoff number
h_f – Heat transfer coefficient
k^* - Mean absorption coefficient
Kn_x – Knudsen number
N_u – Local nusselt number
P_r – Prandtl number
q_r – Radiative heat flux

R_d – Radiation parameter
Re_x - Modified reynolds number
T_f – Temperature of hot fluid
T_∞- Free stream temperature
U_∞ – Uniform velocity

1. INTRODUCTION

The study of non-Newtonian fluid has been of much interest to scientist because some industrial materials are non-Newtonian such as in food, polymer, petrochemical, rubber, paint and biological industries, fluids with non-Newtonian behaviors are encountered. Of particular interest is power-law fluid for which the shear stress τ is given by

$$\tau = \mu\left(\frac{\partial u}{dy}\right) = \mu_0\left(\frac{\partial u}{dy}\right)^n, where\ \mu = \mu_0\left(\frac{\partial u}{dy}\right)^{n-1}$$

Where μ_0 is dynamic coefficient of viscosity, $\frac{\partial u}{\partial y}$ is the shear rate and n is the power-law index. When n <1 the fluid is pseudo-plastic, for n =1 the fluid is Newtonian and for n >1 the fluid is dilatant.

Some examples of a power-law fluid are commercial carboxymethyl cellulose in water, cement rocks in water, napalm in kerosene, lime in water, Illinois yellow clay in water. The studies of the flow of non-Newtonian fluids have over the past years attracted the keen interest of scientist. In response to the pioneering papers of Sakiadis [1], several attempts for further developments in flow and heat transfer analysis have been reported in literature [2-6].

The study of non-Newtonian fluids with or without magnetic field has many applications in industries such as the flow of nuclear fuel slurries, liquid metal and alloys, plasma and mercury, lubrication with heavy oils and greases, coating of papers, polymer extrusion, continuous stretching of plastic films and artificial fibres and many others. The steady viscous incompressible flow of a non-Newtonian power-law fluid on a two-dimensional body in the presence of magnetic fields was studied by Sarpkaya [7]. The flow and heat transfer of a power-law fluid over a uniform moving surface with a constant parallel free stream in the presence of a magnetic field have been studied by Kumari and Nath [8]. Abo-Eldahab and Salem [9] have examined the Hall Effect on the MHD free convection flow of a non-Newtonian power-law fluid on a stretching surface.

In recent years, the study of boundary layer flows of non-Newtonian fluids has increased considerably due to their relevance in scientific and technological applications such as oil recovery, material processing, soil, ceramics, lungs and kidney. In all these situations, one or more extensive quantities are transported through the solid and/or the fluid phases that together occupy a medium. Cheng has studied the natural convection heat and mass transfer of non-Newtonian power-law fluids in porous media [10].

The important experiment by Beavers and Joseph [2] established that when a fluid flows in a parallel plate porous channel, then a velocity slip at the porous wall is proportional to the wall velocity gradient. These observations have led to many publications in non-Newtonian heat and mass transfer, especially the pseudo plastic fluids [11,12]. Kishan and Shashidar Reddy [13] studied the MHD effects on boundary layer flow of power-law fluids past a semi infinite flat plate with thermal dispersion.
Recently Ajadi et al [14] studied the flow and heat transfer of a power law fluid over a flat plate with convective thermal and slip boundary conditions. The purpose of this present work is study the viscous dissipation effects on the flow and heat transfer of a power law fluids in boundary layer over a flat plate using the combination of slip boundary conditions and the convective thermal boundary condition.

2. MATHEMATICAL FORMULATION:

Consider steady two-dimensional boundary layer flows of an incompressible non-Newtonian power-law fluid over a flat plate in a stream of cold fluid at temperature T_∞ moving over the top surface of the flat plate with a uniform velocity U_∞. X-axis is taken along the direction of the flow and Y-axis normal to it.

Also, a magnetic field of strength B is applied in the positive y-direction, which produces magnetic effect in the x-direction. Thus, the continuity, momentum and energy equations describing the flow can be written as

Error! Objects cannot be created from editing field codes.

-----(1)

$$u\frac{\partial u}{\partial x}+v\frac{\partial u}{\partial y}=\nu\frac{\partial}{\partial y}\left(\frac{\partial u}{\partial y}\right)^{n}+g\beta(T-T_\infty)-\frac{\sigma B^2}{\rho}u, \qquad \text{-----(2)}$$

$$\rho c_p\left(u\frac{\partial T}{\partial x}+v\frac{\partial T}{\partial y}\right)=k\frac{\partial^2 T}{\partial y^2}+Q(T-T_\infty)-\frac{\partial q_r}{\partial y}+\mu\left[\frac{\partial u}{\partial y}\right]^{n+1} \qquad \text{-----(3)}$$

The flow velocity boundary conditions associated with this problem can be expressed as

$$u(x,0)=\frac{2-F_M}{F_M}\lambda\frac{\partial u}{\partial y},\ v(x,0)=0 \qquad and \qquad u(x,\infty)=U_\infty \qquad \text{-----(4)}$$

Similarly, assuming that the flat plate is heated from below by a hot fluid whose temperature is maintained at T_f, with heat transfer coefficient h_f, than the boundary condition at the plate surface and beyond the boundary layer may be written as

$$-k\frac{\partial T}{\partial y}(x,0)=h_f[T_f-T(x,0)] \qquad and \qquad T(x,\infty)=T_\infty \qquad \text{-----(5)}$$

Where u and v are velocities along the x-axis (along the plate) and the y-axis (normal to the plate) components respectively, T is the temperature, ν is the kinematic

viscosity of the fluid and k is the coefficient of conductivity of the fluid, q_r is the radiative heat flux, ρ is the density and c_p is the specific heat capacity, Q is the heat source coefficient, B is the magnetic field strength, μ is the magnetic permeability, σ is the electric conductivity, β is the coefficient of thermal expansion, g is the acceleration due to gravity, F_M is the momentum equation accounts for natural convection and the presence of magnetic field, while the energy equation accounts for the heat and radiative sources. By using the Rosseland approximation for radiation, the radiative heat flux may be simplified to be

$$q_r = -\frac{4\sigma^*}{3k^*}\frac{\partial T^4}{\partial y} \qquad \text{-----(6)}$$

Where σ^* and k^* are the Stefan-Boltzmann constant and the mean absorption coefficient respectively. By expressing the term T^4 as a linear function of temperature using the taylor series expansion about T_∞ and neglecting higher-order terms, we get

$$q_r = -\frac{16\sigma^* T_\infty^3}{3k^*}\frac{\partial T}{\partial y} \qquad \text{-----(7)}$$

3. Method of Solution

We shall transform equation (03) and (04) into a set of coupled ordinary differential equation amenable to a numerical solution. For this purpose we introduce a similarity variable η and a dimensionless stream function $f(\eta)$ defined as

$$\left.\begin{aligned} &\eta = y\left(\frac{U_\infty^{2-n}}{\nu x}\right)^{\frac{1}{n+1}} = \frac{y}{x}\mathrm{Re}_x^{\frac{1}{n+1}}, \quad u = U_\infty\frac{\partial f}{\partial \eta} = U_\infty f'(y) \\ &v = \frac{1}{n+1}x^{\frac{-n}{n+1}}\left(U_\infty^{2n-1}\nu\right)^{\frac{1}{n+1}}(\eta f'(\eta) - f(\eta)), \qquad \theta(\eta) = \frac{T-T_\infty}{T_w - T_\infty} \end{aligned}\right\} \qquad \text{-----(8)}$$

Using this in equations (03) & (04), we obtain the following coupled non-linear differential equations.

$$n(f'')^{n-1}f''' + \frac{1}{n+1}f.f'' + G_r\theta - Mf' = 0 \qquad \text{-----(9)}$$

$$\frac{1}{P_r}(1+\frac{4}{3}R_d)\theta'' + \frac{1}{n+1}f\theta' + \gamma\theta + E_c(f'')^{n+1} = 0 \qquad \text{-----(10)}$$

$$\left.\begin{aligned} &f(0) = 0, \qquad f'(0) = \alpha K n_x f''(0), \quad f'(\infty) = 1, \\ &\theta(\infty) = 0, \qquad \theta'(0) = -\phi[1-\theta(0)] \end{aligned}\right\} \qquad \text{-----(11)}$$

Where

$$\mathrm{Re}_x = \frac{x^n U_\infty^{2-n}}{\gamma}, G_r = \frac{g\beta(T_\infty - T_w)x}{U_\infty^2}, M = \frac{\sigma B^2 x}{\rho U_\infty}, R_d = \frac{4\sigma^* T_\infty}{kk^*}, \gamma = \frac{Qx}{\rho c_p U_\infty},$$

$$\varphi = \frac{h_f}{k}\sqrt{\frac{\gamma x}{U_\infty}}, P_r = \frac{\gamma\rho c_p}{kx}\left(\frac{\gamma x}{U_\infty^{2-n}}\right)^{\frac{2}{n+1}}, Kn_x = \frac{\lambda}{x} and \alpha = \frac{F_M - 2}{F_M}.$$

The dimensionless quantities G_r is the Grashoff number, P_r is the Prandtl number, M is the magnetic parameter, Kn_x is the Knudsen number, α is the ratio of accommodation factor, ϕ is the heat transfer coefficient, γ is the heat source parameter and R_d is the radiation parameter.

To solve the system of transformed governing equations (9) & (10) with the boundary conditions (11), we first linearized equation (9) by using Quasi linearization technique[15].

Then equation (9) is transformed to

$$n\left\{[F'']^{n-1}f''' + [f'']^{n-1}F''' - [F'']^{n-1}F'''\right\} + \frac{1}{n+1}[Ff'' + fF'' - FF''] + G_r\theta - Mf' = 0 \quad \text{---(12)}$$

where F is assumed to be a known function and the above equation can be rewritten as

$$A_0 f''' + A_1 f'' + A_3 f' + A_4 f + A_5\theta = A_6 - A_2[f'']^{n-1} \quad \text{-----(13)}$$

where $A_0[i] = n|F''|^{n-1}$, **Error! Objects cannot be created from editing field codes.**, **Error! Objects cannot be created from editing field codes.**,

$$A_3[i] = M, \qquad A_4[i] = \frac{1}{n+1}F'', \qquad A_5[i] = G_r,$$

$$A_6[i] = n[F'']^{n-1}F''' + \frac{1}{n+1}FF''$$

Equation (11) is expressed is the simplified form as

$$B_0\theta'' + B_1\theta' + B_2\theta + B_3 = 0, \quad \text{-----(14)}$$

Where

$$B_0[i] = 1 + \frac{4}{3}R_d, \quad B_1[i] = \frac{1}{n+1}P_r f, \quad B_3[i] = \gamma P_r, \quad B_4[i] = Ec[f'']^{n+1},$$

Using implicit finite difference formulae, the equations (13) & (14) are transformed to

$$C_0[i]f[i+2] + C_1[i]f[i+1] + C_2[i]f[i] + C_3[i]f[i-1] + C_4[i]\theta[i] = C_5[i] \quad \text{-----(15)}$$

And

$$D_0[i]\theta[i+1] + D_1[i]\theta[i] + D_2[i]\theta[i-1] + D_3[i] = 0, \quad \text{-----(16)}$$

Where

$C_0[i] = 2A_0[i]$ $C_1[i] = -6A_0[i] + 2hA_1[i] + h^2A_3[i]$

$C_2[i] = 6A_0[i] - 4hA_1[i] + 2h^3A_4[i]$ $C_3[i] = -2A_0[i] + 2hA_1[i] - h^2A_3[i]$

$C_4[i] = 2h^3A_5[i]$ $C_5[i] = 2h^3\{ A_6[i] - A_2 [F''[i]]^{n-1}\}$

and

$D_0[i] = 2B_0[i] + h B_1[i]$ $D_1[i] = -4B_0[i] + 2h^2B_2[i]$

$D_2[i] = 2B_0[i] - hB_1[i]$ $D_3[i] = 2h^2B_3[i]$

here 'h' represents the mesh size in η direction. Equation (15) & (16) are solved under the boundary conditions (11) by Thomas algorithm and computations were carried out by using C programming. The numerical solutions of f are considered as $(n+1)^{th}$ order iterative solutions and F are the n^{th} order iterative solutions. After each cycle of iteration the convergence check is performed, and the process is terminated when $|F - f| < 10^{-6}$.

4. SKIN FRICTION

The shearing stress on the surface is defined by

$$\tau_w = \mu \left.\frac{\partial u}{\partial y}\right|_{y=0} \qquad \text{-----(17)}$$

Thus the skin friction coefficient is defined by

$$C_f = \frac{2\tau_w}{\rho U_\infty} = 2\,\mathrm{Re}_x^{\frac{-1}{n+1}}\left[f''(0)\right]^n, \qquad \text{-----(18)}$$

5. HEAT TRANSFER

The local Nusselt number for heat transfer is defined by

$$N_u = \frac{\nu q_w}{k(T_\infty - T_w)} = -\nu x^{-1}\,\mathrm{Re}_x^{\frac{1}{n+1}}\,\theta'(0), \qquad \text{-----(19)}$$

Where the heat flux at the wall is given by $q_w = -k \left.\frac{\partial T}{\partial y}\right|_{y=0}$

6. RESULTS AND DISCUSSIONS

In order to carryout subsequent analysis of the effects of different flow parameters and to investigate the influence power-law indexes of non-Newtonian fluids over a flat plate with thermal boundary condition, numerical solutions are obtained for $f'(\eta)$, $\theta(\eta)$ and $\theta'(\eta)$ for the different flow parameters Knudsen number Kn_x, Heat transfer coefficient ϕ, magnetic field parameter M, power-law index n, Eckert number E_c and Prandtl number P_r. With the knowledge of $f'(\eta)$, $\theta(\eta)$ and $\theta'(\eta)$ the skin friction coefficient $f''(0)$, temperature $\theta(0)$ and the rate of heat transfer coefficient $\theta'(0)$ are computed.

Numerical values are tabulated for $f''(0)$, $\theta(0)$, $\theta'(0)$ for various values of Knudsen number Kn_x, Heat transfer coefficient ϕ and Eckert number E_c for both pseudo plastic (n = 0.5) and Newtonian fluid (n = 1.0) in Tables 1-6. Table 1 and 4 shows that the skin friction coefficient $f''(0)$ decreases with the increase in the Knudsen number Kn_x whereas, it has no effect with the change in heat transfer coefficient ϕ and Eckert number E_c which is shown in tables 2,3, 5 and 6 for both pseudo-plastic (n = 0.5) and Newtonian fluids (n = 1.0). It is seen that the values of skin friction coefficient are higher for pseudo-plastic fluids (n = 0.5) than the Newtonian fluids (n = 1.0). From tables 1 and 4 show that temperature at the wall $\theta(0)$ decrease with the increase in the Knudsen number Kn_x with and without radiation. The temperature at the wall $\theta(0)$ value increases with the increase in the heat transfer coefficient ϕ and Eckert number E_c for both pseudo-plastic (n =0.5) and Newtonian fluids (n = 1.0) which is shown in tables 2, 3, 5 and 6. The variation of $-\theta'(0)$ with Kn_x and ϕ are shown in tables 1,2, 4 and 5 . It is evident from the tables that $-\theta'(0)$ value increases with the effect of Kn_x and ϕ for both pseudo-plastic (n = 0.5) and Newtonian fluids (n =1.0). From the tables 3 and 6 it is seen that effect of Eckert number E_c is to decrease $-\theta'(0)$ value for both pseudo-plastic (n =0.5) and Newtonian fluids (n = 1.0).

Table 1: M = 0.1, γ = 0.1, ϕ = 1, **n = 0.5**, G_r = 0, Ec = 0.0

Kn_x	$f''(0)$	R_d = 0, P_r = 0.72		R_d = 10, P_r = 0.72		R_d = 10, P_r = 10	
		$\theta(0)$	$-\theta'(0)$	$\theta(0)$	$-\theta'(0)$	$\theta(0)$	$-\theta'(0)$
0	0.163284	0.869726	0.130274	0.902856	0.097144	0.868952	0.131048
1	0.154233	0.842309	0.157691	0.899305	0.100695	0.836174	0.163826
2	0.142576	0.823169	0.176831	0.896657	0.103343	0.813641	0.186359
3	0.130896	0.809406	0.190594	0.894662	0.105338	0.797607	0.202393
4	0.120207	0.799132	0.200868	0.893122	0.106878	0.785726	0.214274
5	0.110753	0.791188	0.208812	0.891900	0.108100	0.776592	0.223408
6	0.102491	0.784859	0.215141	0.890906	0.109094	0.769347	0.230653
7	0.095278	0.779689	0.220311	0.890080	0.109920	0.763449	0.236551

Table 2: M = 0.1, γ = 0.1, Kn_x = 1, **n = 0.5**, G_r = 0, Ec = 0.0

ϕ	$f''(0)$	R_d = 0, P_r = 0.72		R_d = 10, P_r = 0.72		R_d = 10, P_r = 10	
		$\theta(0)$	$-\theta'(0)$	$\theta(0)$	$-\theta'(0)$	$\theta(0)$	$-\theta'(0)$
0.1	0.154233	0.348174	0.065183	0.471766	0.052823	0.337926	0.066207
0.2	0.154233	0.516513	0.096697	0.641089	0.071782	0.505149	0.098970
0.4	0.154233	0.681184	0.127526	0.781297	0.087481	0.671228	0.131509
0.6	0.154233	0.762183	0.14269	0.842733	0.094360	0.753842	0.147695
0.8	0.154233	0.810363	0.15171	0.877222	0.098222	0.803275	0.157380
1.0	0.154233	0.842309	0.157691	0.899305	0.100695	0.836174	0.163826
1.5	0.154233	0.889040	0.166439	0.930530	0.104192	0.884474	0.173289
2.0	0.154233	0.914406	0.171188	0.946983	0.106033	0.910779	0.178442

Table 3: M = 0.1, γ = 0.1, Kn_x = 1,ϕ = 1, **n = 0.5**, G_r = 0

Ec	$f''(0)$	R_d = 0, P_r = 0.72		R_d = 10, P_r = 0.72		R_d = 10, P_r = 10	
		$\theta(0)$	$-\theta'(0)$	$\theta(0)$	$-\theta'(0)$	$\theta(0)$	$-\theta'(0)$
0.0	0.154233	0.842309	0.157691	0.899315	0.100695	0.836174	0.163826
0.5	0.154233	0.994118	0.005882	0.917458	0.082542	0.849477	0.150523
1.0	0.154233	1.145928	-0.14593	0.935612	0.064388	0.862779	0.137221
2.0	0.154233	1.449540	-0.44954	0.971918	0.028082	0.889385	0.110615
5.0	0.154233	2.360401	-1.3604	1.080837	-0.08084	0.969200	0.030800
10	0.154233	3.878493	-2.87849	1.262369	-0.26237	1.102226	-0.10223
20	0.154233	6.914677	-5.91468	1.625432	-0.62543	1.368278	-0.36828

Table 4 : M = 0.1, γ = 0.1, ϕ = 1, **n = 1.0**, G_r = 0, Ec = 0.0

Kn_x	$f''(0)$	R_d = 0, P_r = 0.72		R_d = 10, P_r = 0.72		R_d = 10, P_r = 10	
		$\theta(0)$	$-\theta'(0)$	$\theta(0)$	$-\theta'(0)$	$\theta(0)$	$-\theta'(0)$
0	0.130829	0.922079	0.077921	0.911301	0.088698	0.929168	0.070832
1	0.122689	0.897537	0.102463	0.908968	0.091032	0.898810	0.101190
2	0.113236	0.880278	0.119721	0.907202	0.092798	0.877825	0.122175
3	0.103921	0.867827	0.132173	0.905862	0.094138	0.862857	0.137143
4	0.095364	0.858572	0.141428	0.904830	0.095170	0.851817	0.148183
5	0.087740	0.851490	0.148510	0.90402	0.09598	0.848419	0.156581
6	0.081031	0.845928	0.154072	0.903371	0.096629	0.836851	0.163149

Table 5 : M = 0.1, γ = 0.1, Kn_x = 1, **n = 1.0**, G_r = 0, Ec = 0.0

ϕ	$f''(0)$	R_d = 0, P_r = 0.72		R_d = 10, P_r = 0.72		R_d = 10, P_r = 10	
		$\theta(0)$	$-\theta'(0)$	$\theta(0)$	$-\theta'(0)$	$\theta(0)$	$-\theta'(0)$
0.1	0.122689	0.466941	0.053306	0.499630	0.050037	0.470406	0.052959
0.2	0.122689	0.636619	0.072676	0.666338	0.066732	0.639831	0.072034
0.4	0.122689	0.777968	0.088813	0.799763	0.080095	0.780362	0.087855
0.6	0.122689	0.840148	0.095911	0.856961	0.085823	0.842008	0.094795
0.8	0.122689	0.875120	0.099904	0.888743	0.089006	0.876633	0.098693
1.0	0.122689	0.897537	0.102463	0.908968	0.091032	0.898810	0.101190
1.5	0.122689	0.929276	0.106086	0.937413	0.093880	0.930185	0.104723
2.0	0.122689	0.946002	0.107996	0.952314	0.095372	0.946709	0.106583

Table 6 : M = 0.1, γ = 0.1, Kn_x = 1, ϕ = 1, **n = 1.0**, G_r = 0

Ec	$f''(0)$	R_d = 0, P_r = 0.72		R_d = 10, P_r = 0.72		R_d = 10, P_r = 10	
		$\theta(0)$	$-\theta'(0)$	$\theta(0)$	$-\theta'(0)$	$\theta(0)$	$-\theta'(0)$
0.0	0.122689	0.897537	0.102463	0.908968	0.091032	0.898810	0.101190
0.5	0.122689	0.955540	0.044460	0.914936	0.085064	0.903990	0.096010
1.0	0.122689	1.013543	-0.01354	0.920903	0.079097	0.909171	0.090829
2.0	0.122689	1.129548	-0.12955	0.932838	0.067162	0.919532	0.080468
5.0	0.122689	1.477564	-0.47756	0.968641	0.031359	0.950616	0.049384
10.0	0.122689	2.057592	-1.05759	1.028314	-0.02831	1.002422	-0.00242
20.0	0.122689	3.217648	-2.21765	1.147661	-0.14766	1.106034	-0.10603

6.1 Influence of Knudsen number Kn_x

Figures 1 and 2 show that the dimensionless velocity profiles $f'(\eta)$ increases with the increase of Knudsen number Kn_x for both pseudo-plastic (n = 0.5) and Newtonian fluids (n = 1.0) for fixed values of radiation parameter R_d = 0 and R_d = 10. It is evident from these figures that the thermal boundary layer becomes thinner as Kn_x increases. The effect of Knudsen number Kn_x on the temperature profiles is shown in the figures 5 and 6, from which is observed that the temperature profiles decrease with the increase in Knudsen number Kn_x for both the cases of pseudo-plastic (n = 0.5) and Newtonian fluids (n = 1.0) for fixed values of radiation parameter R_d = 0 and R_d = 10. It is noticed form the figures that the temperature profiles are higher in the presence of radiation parameter with R_d = 10 when compared to R_d = 0.

The effect of Knudsen number Kn_x is very less in presence of radiation parameter for Newtonian fluids. Figures 13 and 14 were drawn for temperature profiles $\theta'(\eta)$ for pseudo-plastic (n = 0.5) and Newtonian fluids (n = 1.0) with and without radiation parameter. With the increase of Knudsen number Kn_x $\theta'(\eta)$ decreases near the boundary layer upto a certain extent and there after it will increase for both the cases of pseudo-plastic (n = 0.5) and Newtonain fluids (n = 1.0) in the absence of radiation

parameter. And in the presence of radiation parameter R_d = 10 with the increase in Knudsen number Kn_x it decreases near the boundary layer while it increases far away from the boundary.

6.2 Influence of Heat transfer coefficient

Figure 3 show that with the effect of heat transfer coefficient ϕ there is no variation in velocity profile $f'(\eta)$ for both pseudo-plastic (n = 0.5) and Newtonian fluids (n = 1.0) . The influence of heat transfer coefficient ϕ is to increase the temperature profile $\theta(\eta)$ for fixed values of radiation parameter R_d = 0 and R_d = 10 in the both the cases of pseudo-plastic (n = 0.5) and Newtonian fluids (n = 1.0) which is shown in figures 7 and 8.

Figures 15 and 16 are drawn for temperature profile $\theta'(\eta)$ for various values of heat transfer coefficient ϕ in both the cases of pseudo-plastic (n = 0.5) and Newtonian fluids (n = 1.0) with and without radiation. It can be seen that the effect of heat transfer coefficient ϕ is to reduce the temperature profiles $\theta'(\eta)$ in all the cases. It is observed that $\theta'(\eta)$ is zero always in the absence of heat transfer coefficient ϕ.

6.3 Influence of Magnetic field

The effect of magnetic field on the velocity profiles $f'(\eta)$ is shown in the figure 4. It is evident from the figure that the magnetic field effect is to decelerate the velocity profiles $f'(\eta)$ for both the cases of pseudo-plastic (n = 0.5) and Newtonian fluids (n = 1.0) in the absence of radiation parameter R_d.

6.4 Influence of Power-law index

It can be shown from the figure 9 that the influence of power-law index n is to reduce the velocity profile $f'(\eta)$. Whereas from the figure 10 it can be noticed that the temperature profiles $\theta(\eta)$ increases with the increase in the power-law index n.

6.5 Influence of Viscous Dissipation

The influence of viscous dissipation on temperature profile $\theta(\eta)$ is shown in figures 11 and 12. It is observed from the figures that temperature profiles increases with the increase of Eckert number E_c in both the cases of pseudo-plastic (n = 0.5) and Newtonian fluids (n = 1.0) with and without radiation. It is also noticed that viscous dissipation effect is more in pseudo-plastic fluids (n = 0.5) when compared with the Newtonian fluids (n = 1.0). And It is seen that this effect is very less in the presence of radiation (R_d= 10). The effect of viscous dissipation on temperature profiles $\theta'(\eta)$ is shown in figures 17 and 18. The viscous dissipation effect is to increase the temperature profiles $\theta'(\eta)$ near the plate whereas a reverse phenomenon could be seen far away from the plate for both the cases of pseudo-plastic (n = 0.5) and Newtonian fluids (n = 1.0) with and without radiation.

6.6 Influence of Prandtl number

The influence of prandtl number on the dimensionless temperature profile $\theta'(\eta)$ for pseudo-plastic fluids (n = 0.5) is shown in figure 19. It is seen from that temperature profiles $\theta'(\eta)$ decreases near the thermal boundary layer and it increases after certain distance with increase in the prandtl number. It is noticed that at far away from the plate $\theta'(\eta)$ is zero.

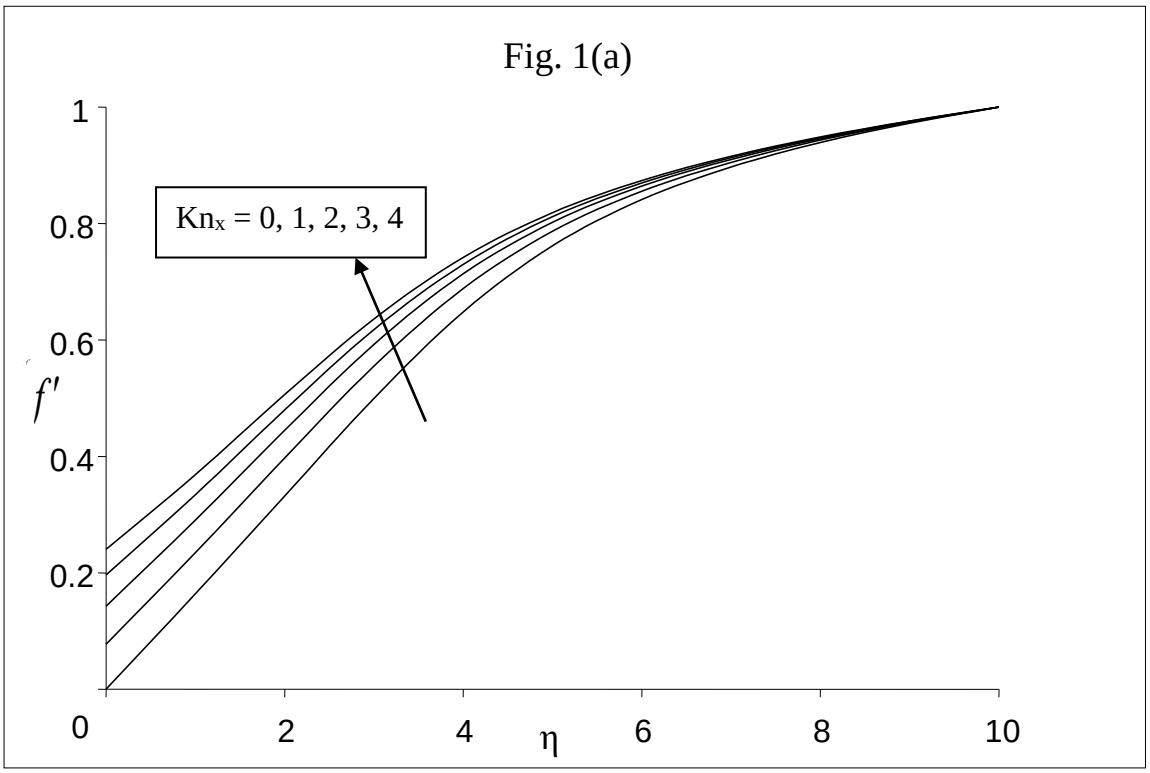

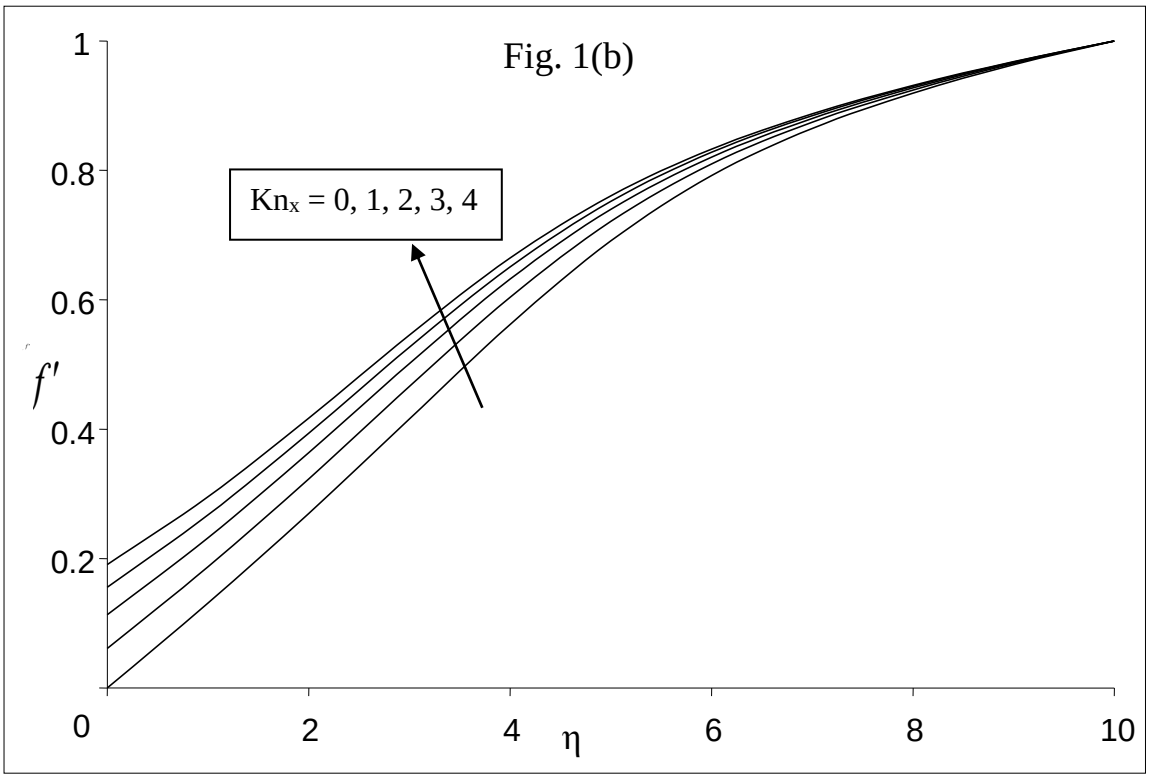

Fig. 1 Velocity profiles for various values of Knudsen number Kn_x with $\phi = 1$, $P_r = 0.72$, $R_d = 0$ and $M = 0.1$. **(a)** n = 0.5 **(b)** n = 1.0

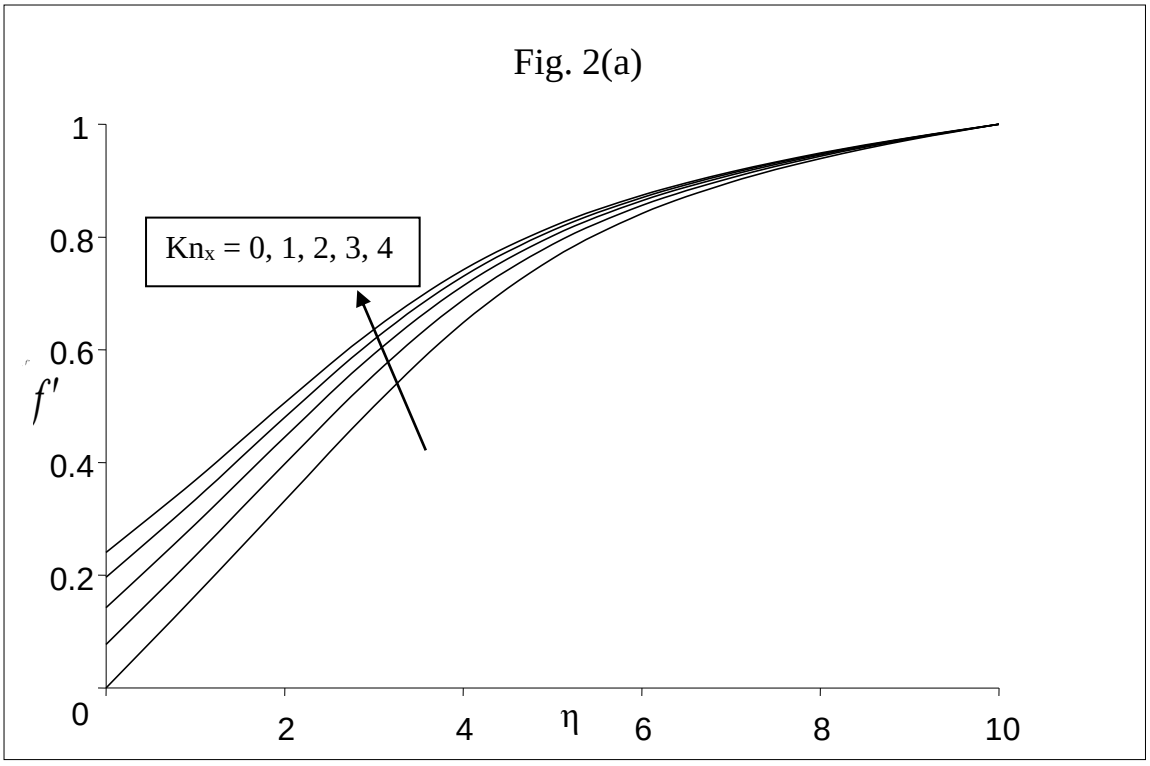

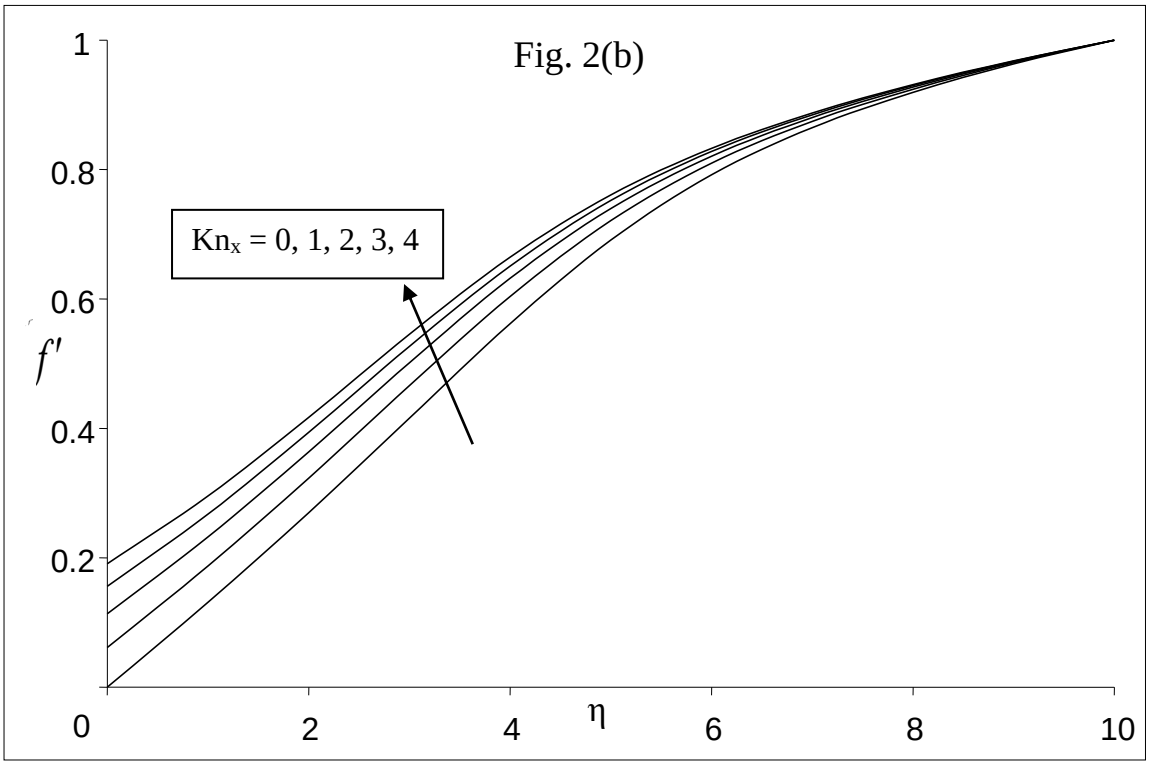

Fig. 2 Velocity profiles for various values of Knudsen number Kn_x with $\phi = 1$, $P_r = 0.72$, $R_d = 10$ and $M = 0.1$. **(a)** n = 0.5 **(b)** n = 1.0

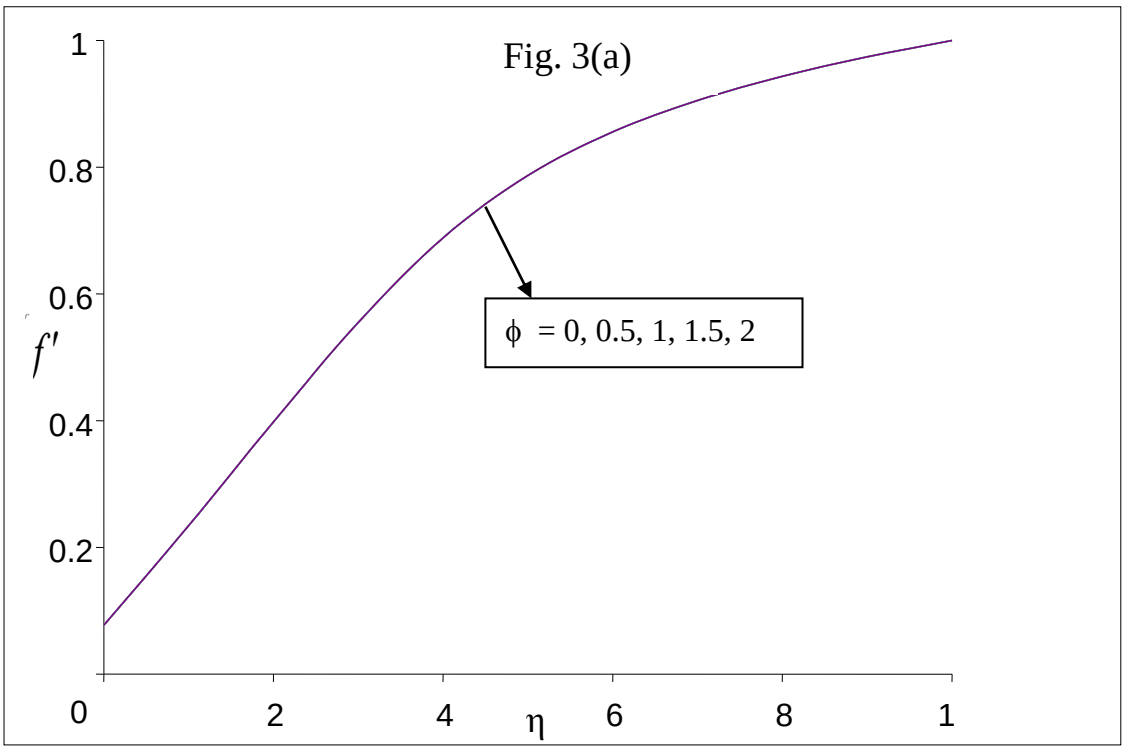

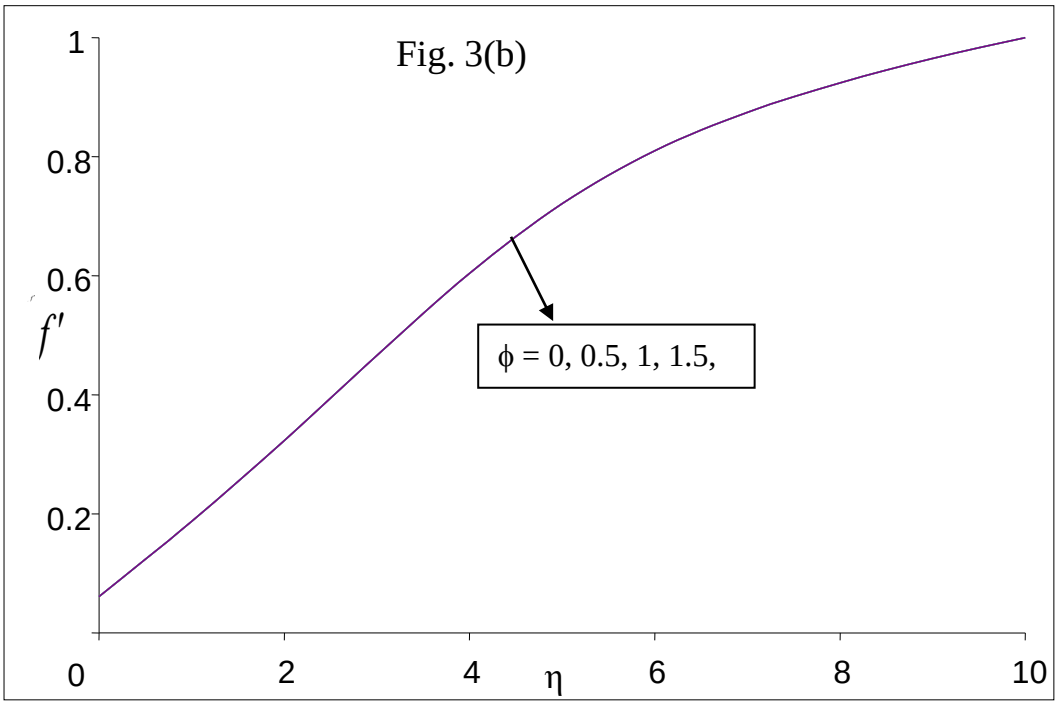

Fig. 3 Velocity profiles for various values of heat transfer coefficient ϕ with $Kn_x = 1$, P_r=0.72, R_d = 0 and M = 0.1. **(a)** n = 0.5 **(b)** n = 1.0

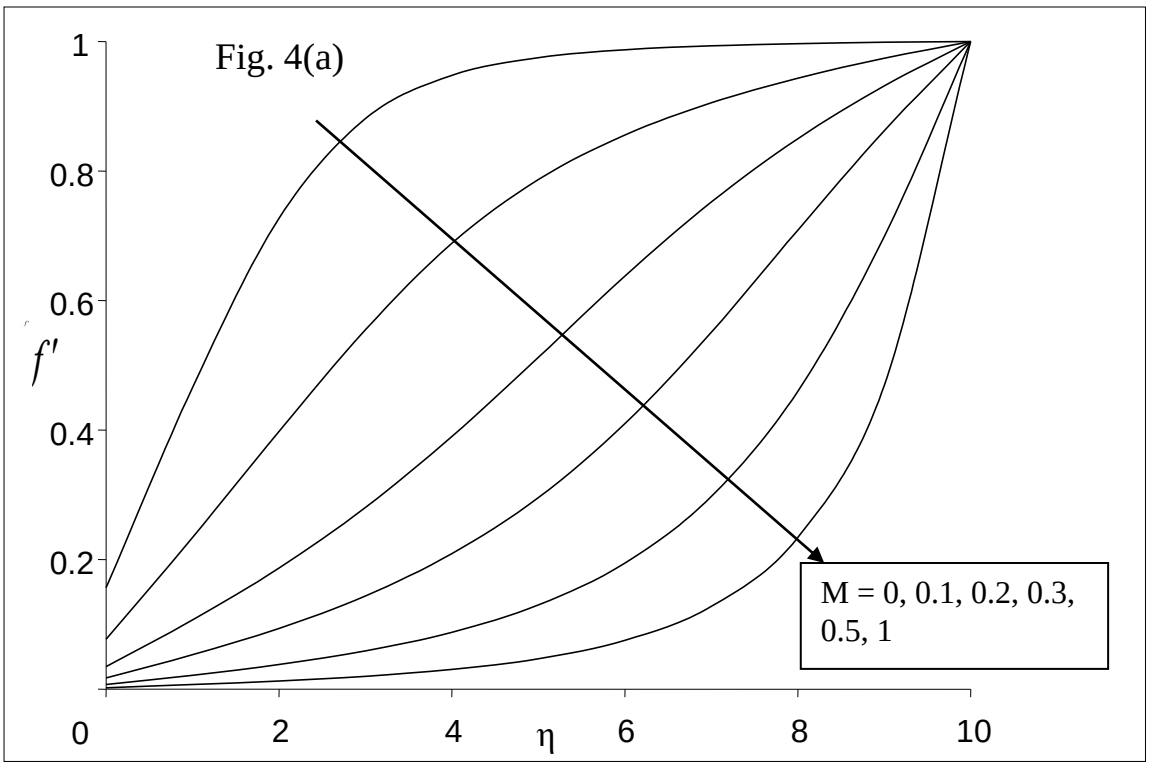

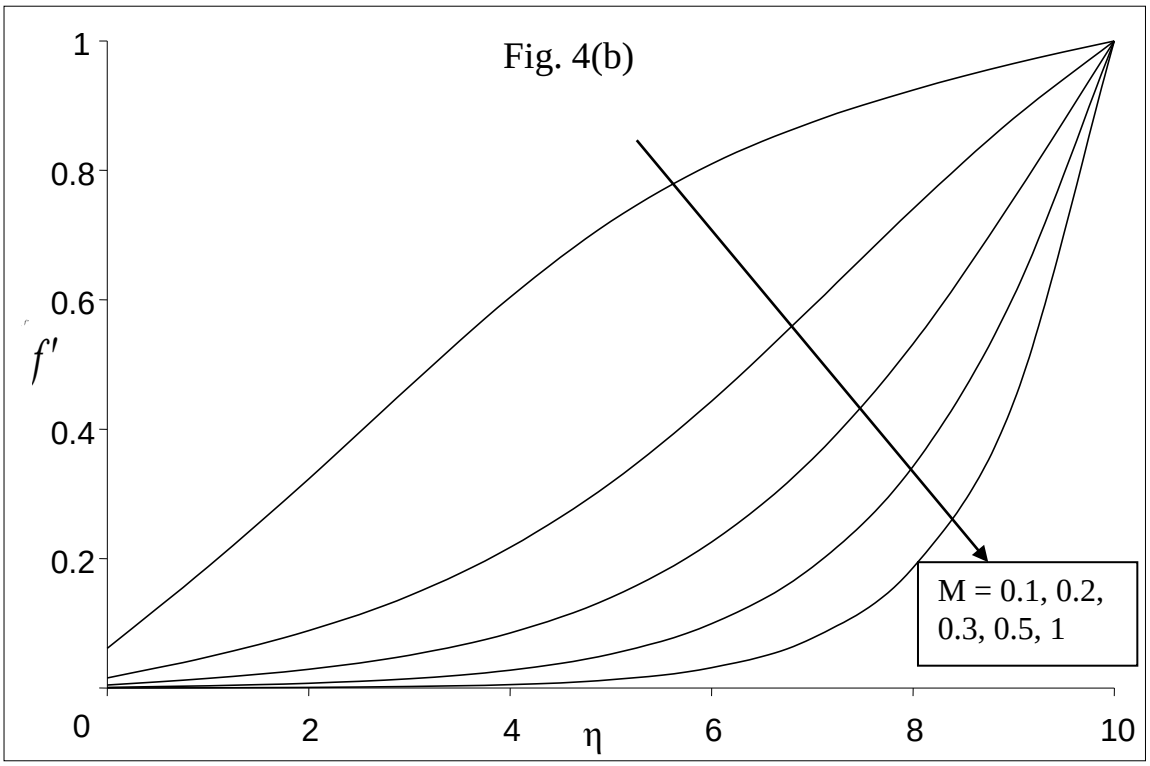

Fig. 4 Velocity profiles for various values of Magnetic parameter M with $Kn_x = 1$, $\phi = 1$, $R_d = 0$ and $P_r = 0.72$ **(a)** n = 0.5 **(b)** n = 1.0

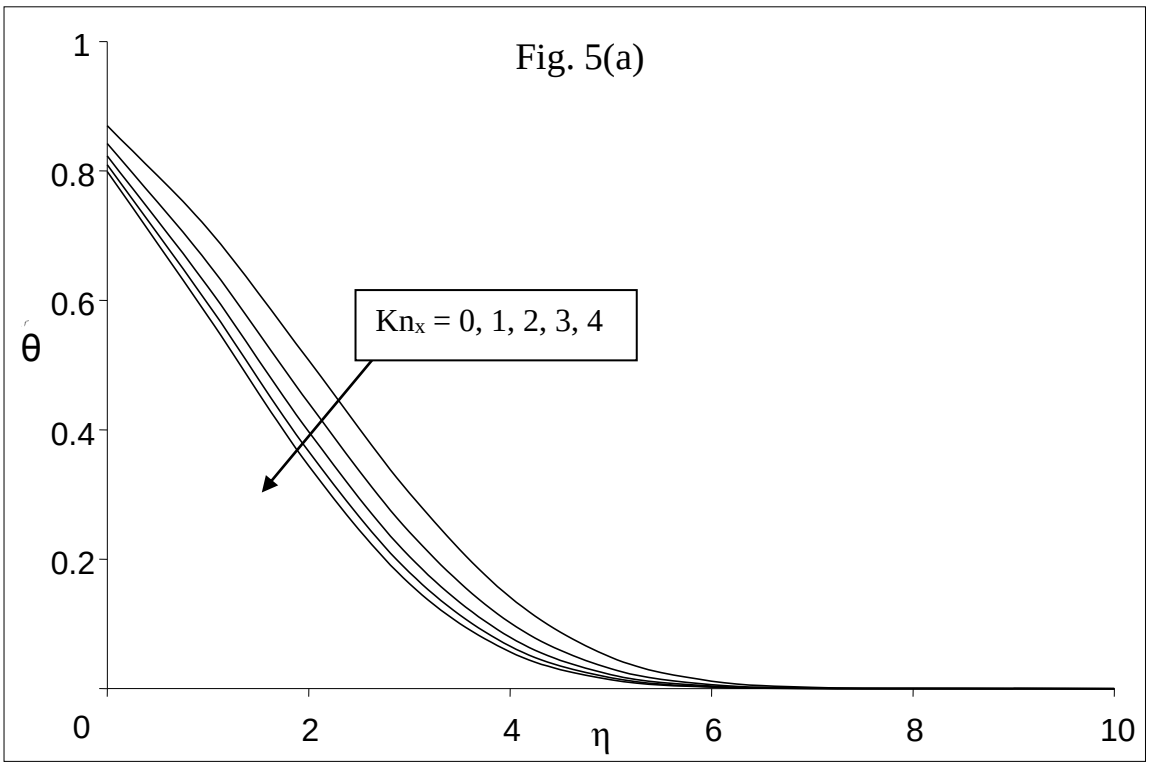

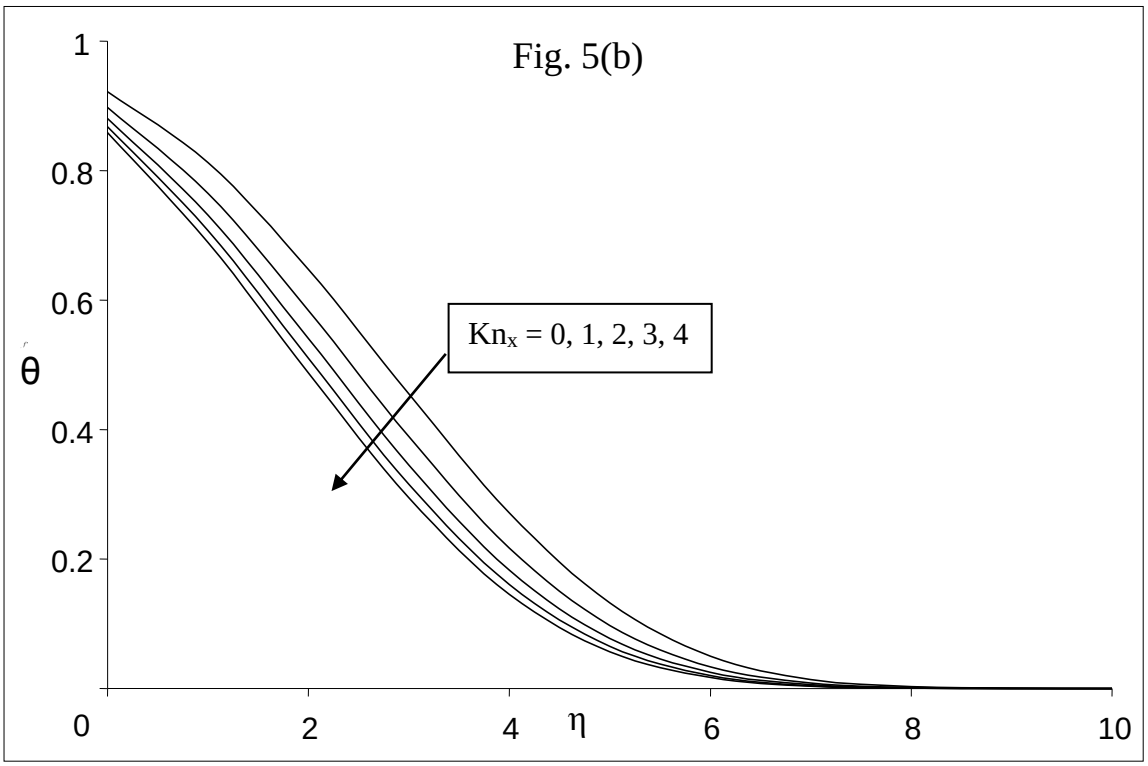

Fig. 5 Temperature profiles for various values of Knudsen number Kn_x with $\phi = 1$, P_r=0.72, $R_d = 0$, $E_c = 0$ and M = 0.1 **(a)** n = 0.5 **(b)** n = 1.0

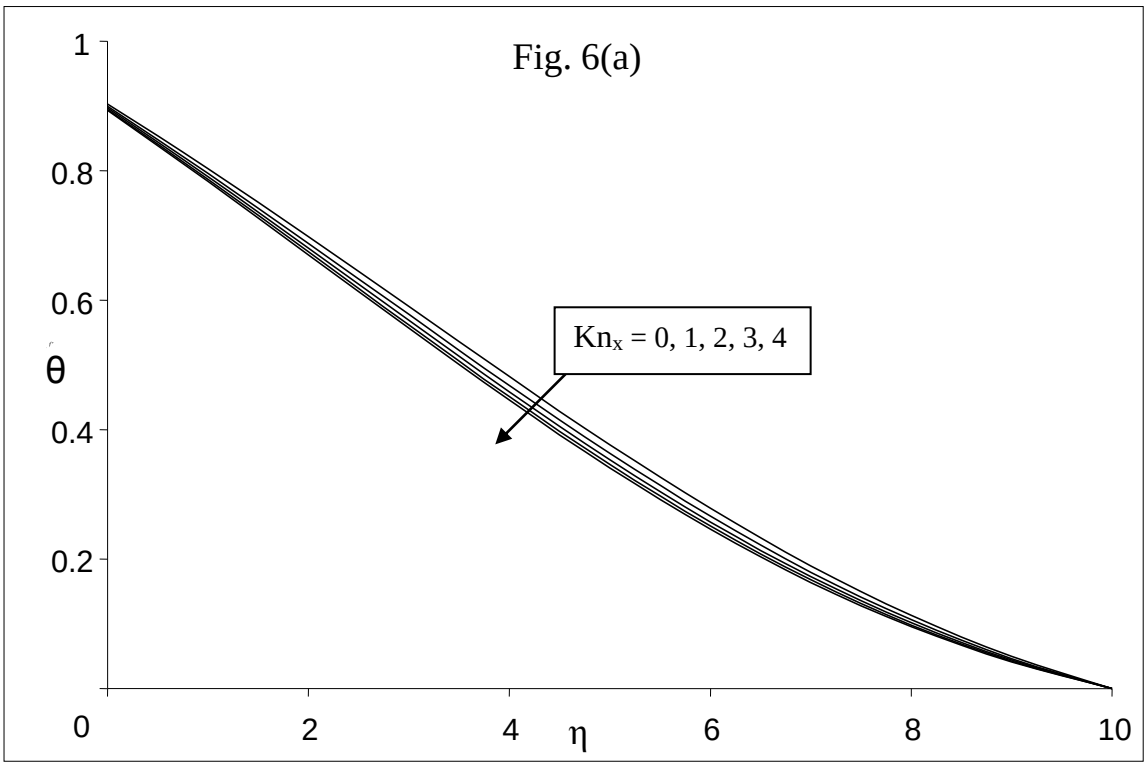

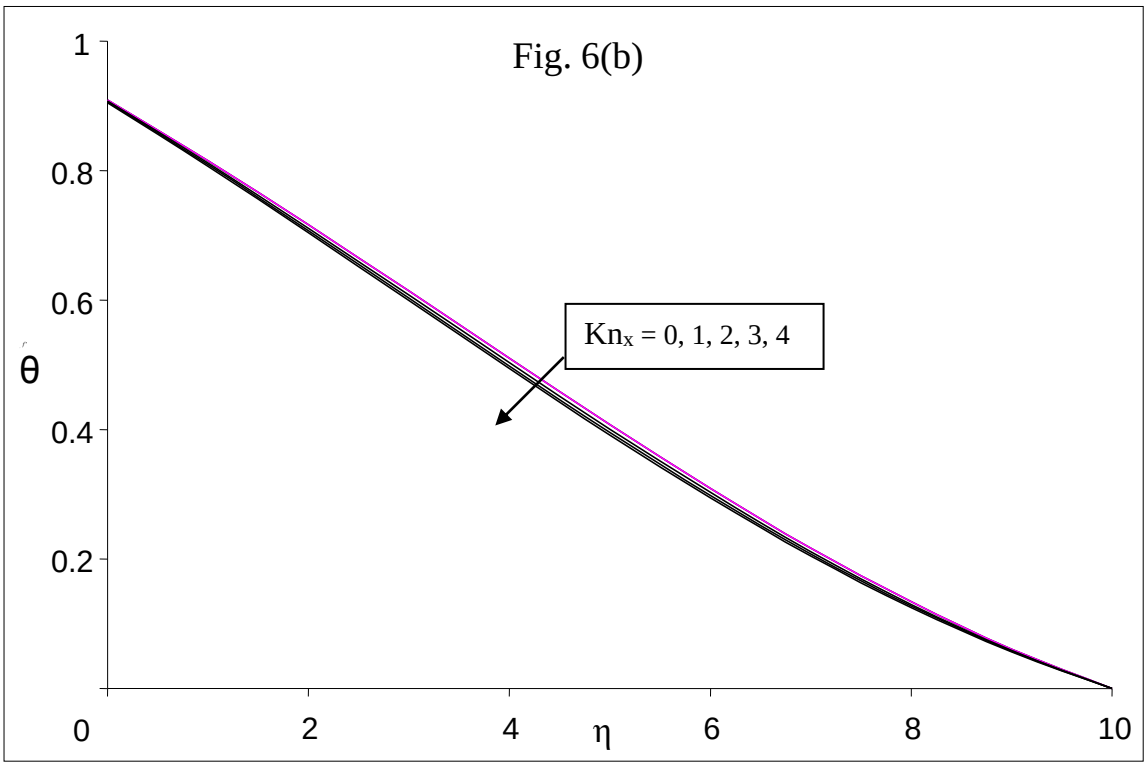

Fig. 6 Temperature profiles for various values of Knudsen number Kn_x with $\phi = 1$, P_r=0.72, $R_d = 10$, $E_c = 0$ and M = 0.1 **(a)** n = 0.5 **(b)** n = 1.0

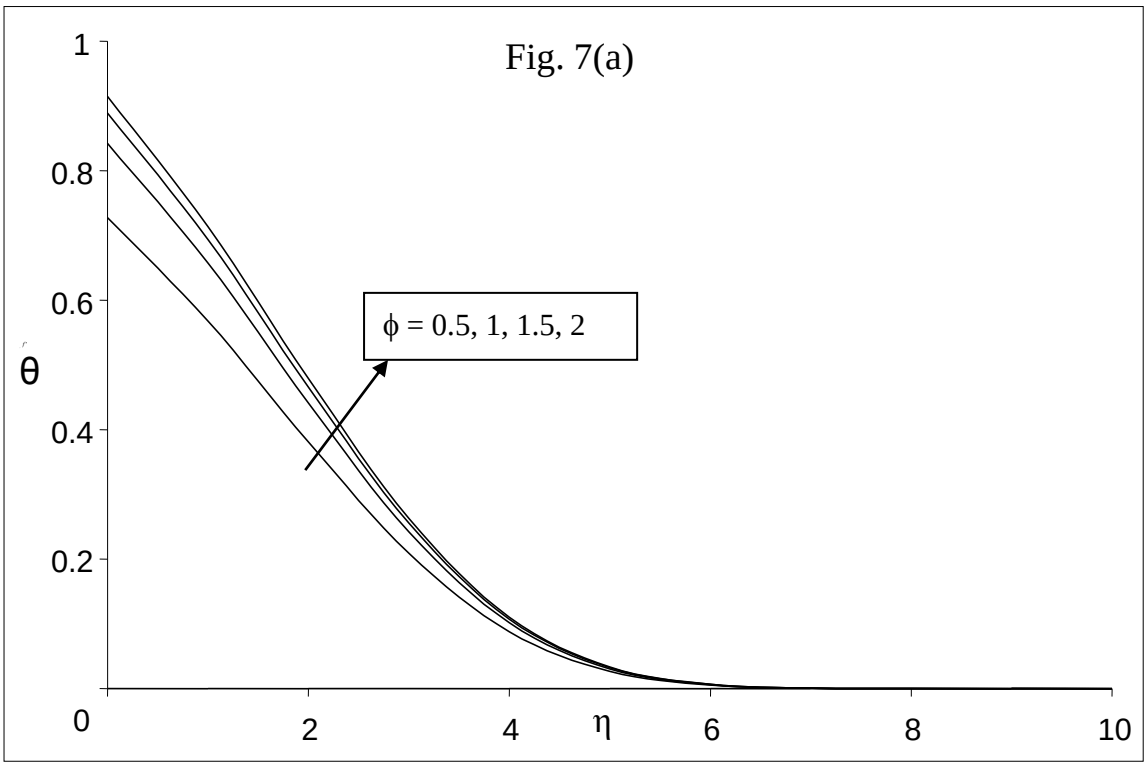

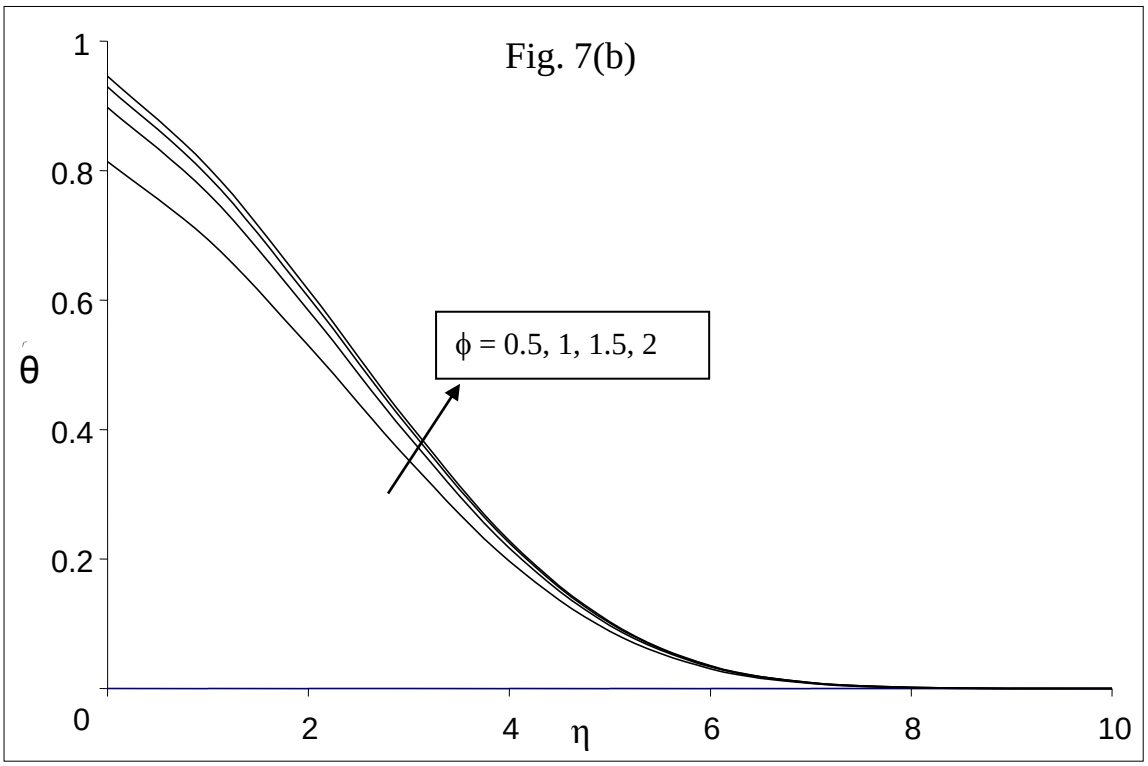

Fig. 7 Temperature profiles for various values of heat transfer coefficient ϕ with Kn_x = 1, P_r = 0.72, R_d = 0, E_c = 0 and M = 0.1 **(a)** n = 0.5 **(b)** n = 1.0

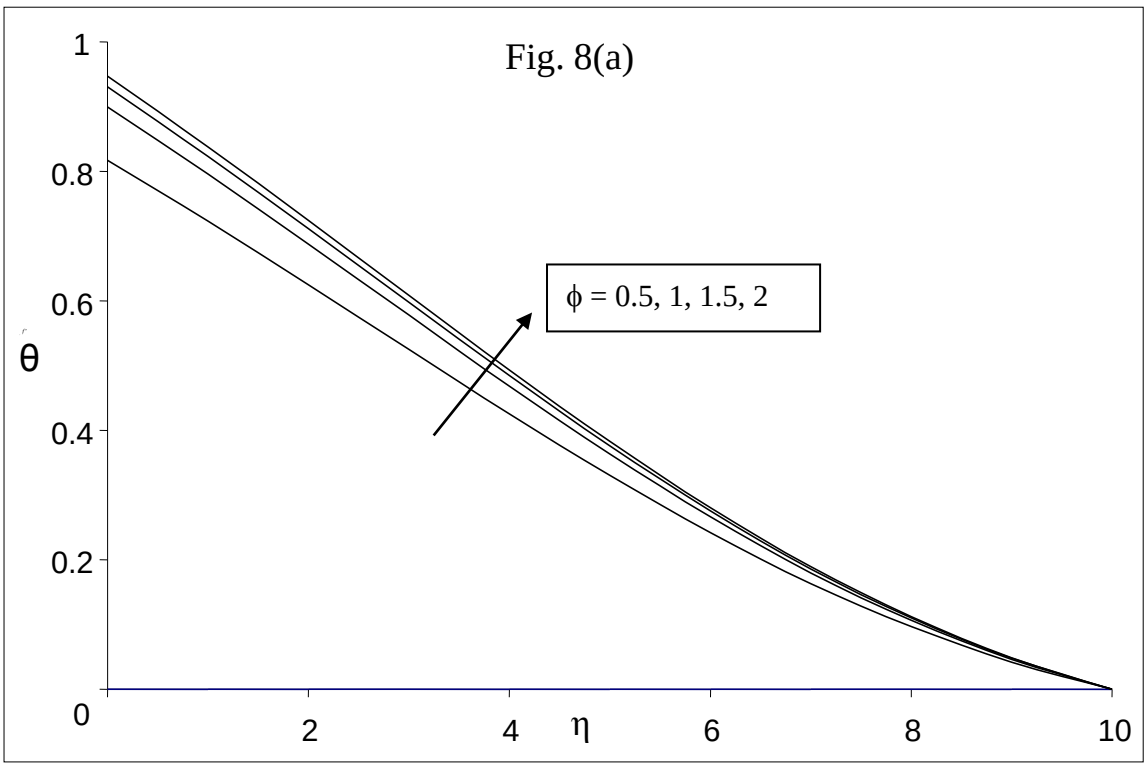

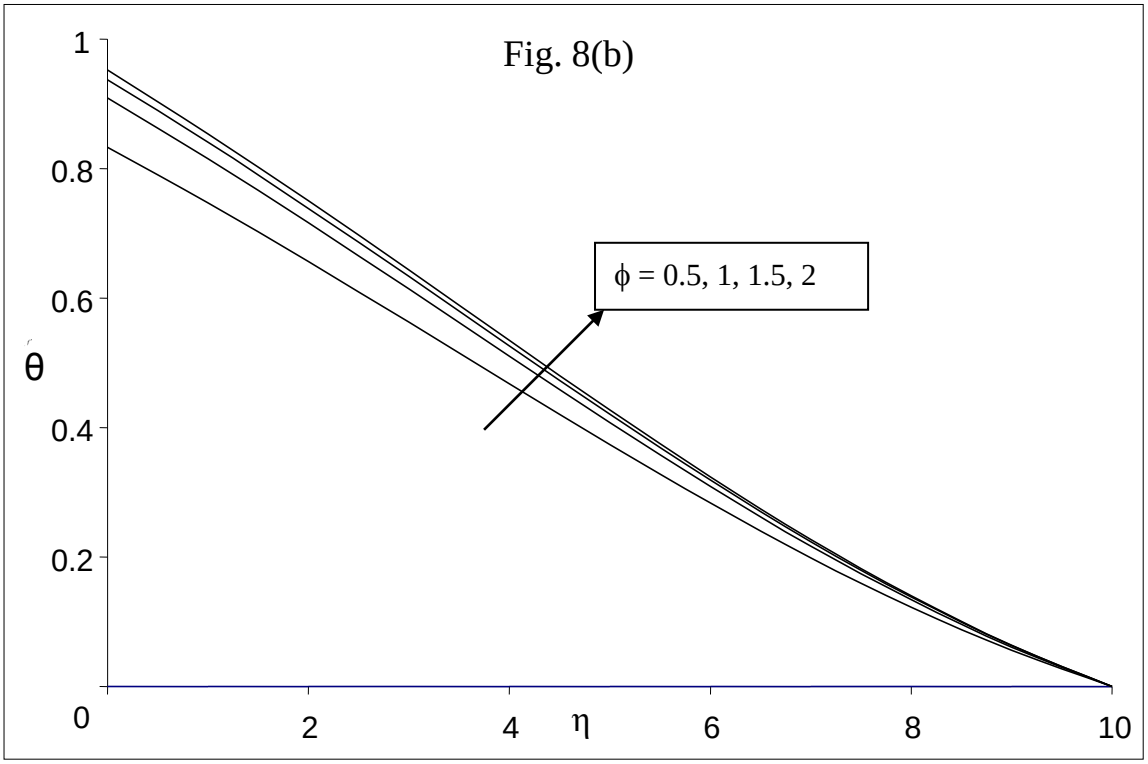

Fig. 8 Temperature profiles for various values of heat transfer coefficient ϕ with Kn_x = 1, P_r = 0.72, R_d = 10, E_c = 0 and M = 0.1 **(a)** n = 0.5 **(b)** n = 1.0

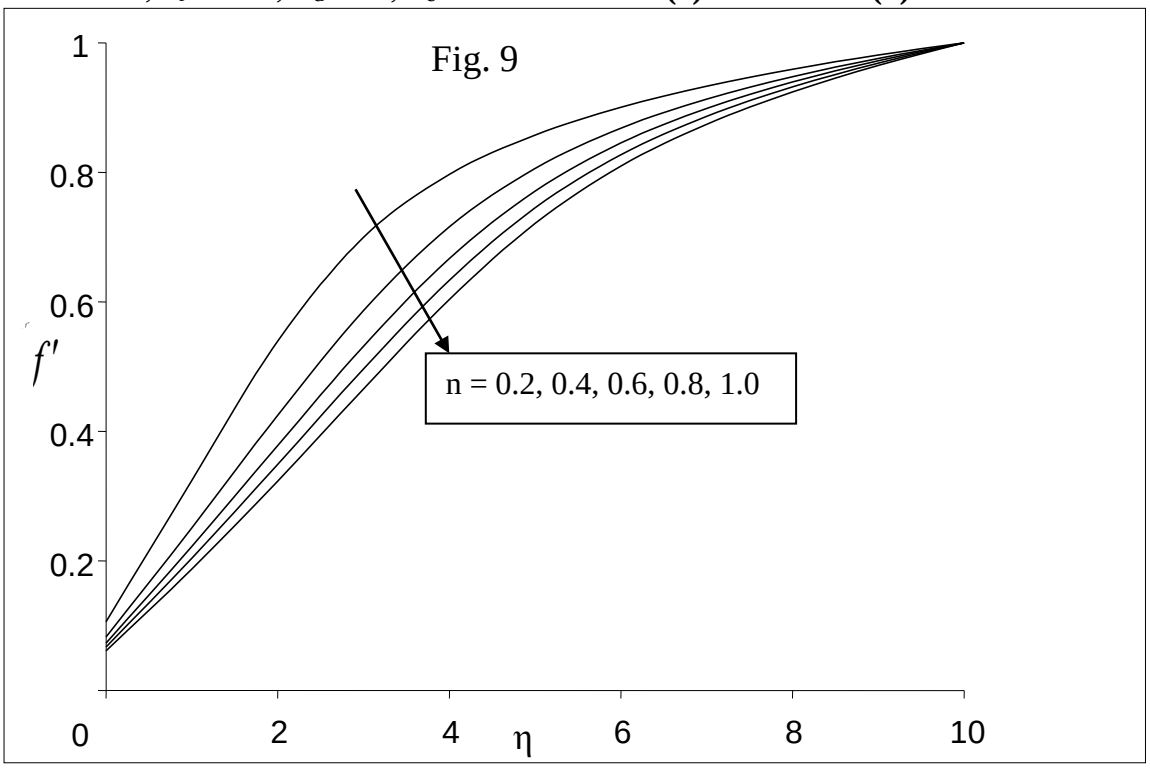

Fig. 9 Velocity profiles for various values of power law index n with Kn_x = 1, ϕ = 1, P_r=0.72, R_d = 10 and M = 0.1.

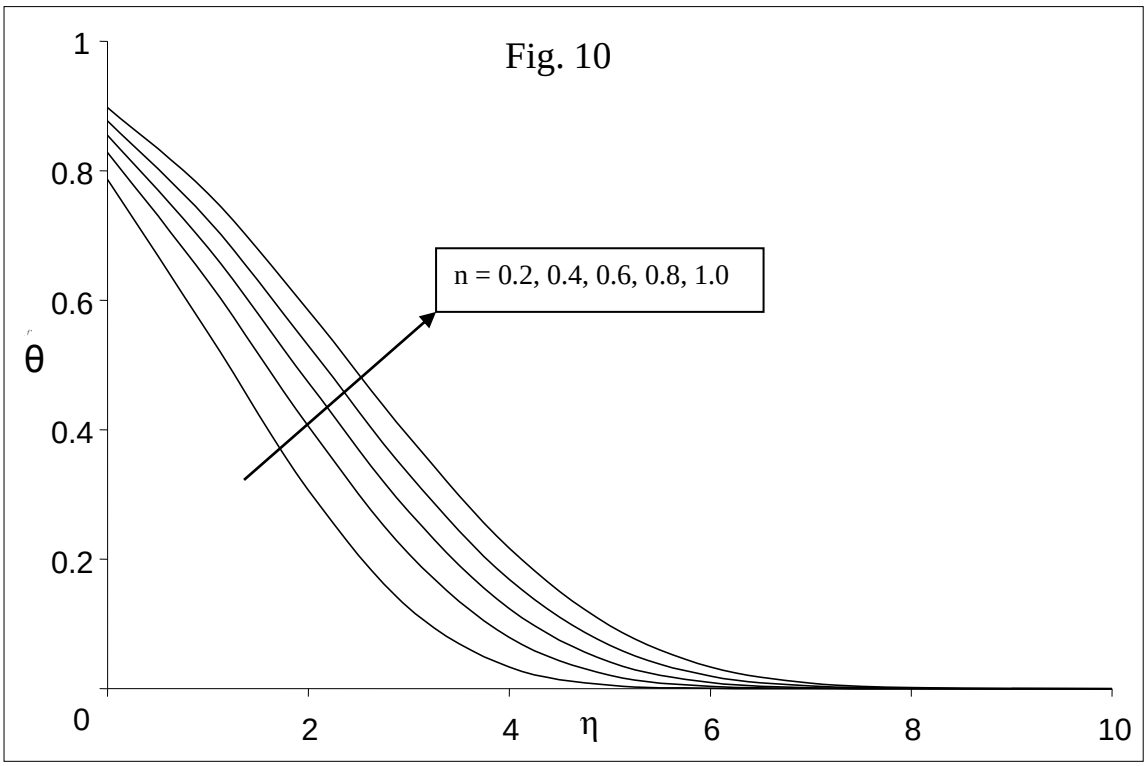

Fig. 10 Temperature profiles for various values of power law index n with $Kn_x = 1$, $\phi = 1$, $P_r=0.72$, $R_d = 10$ $E_c = 0$ and $M = 0.1$.

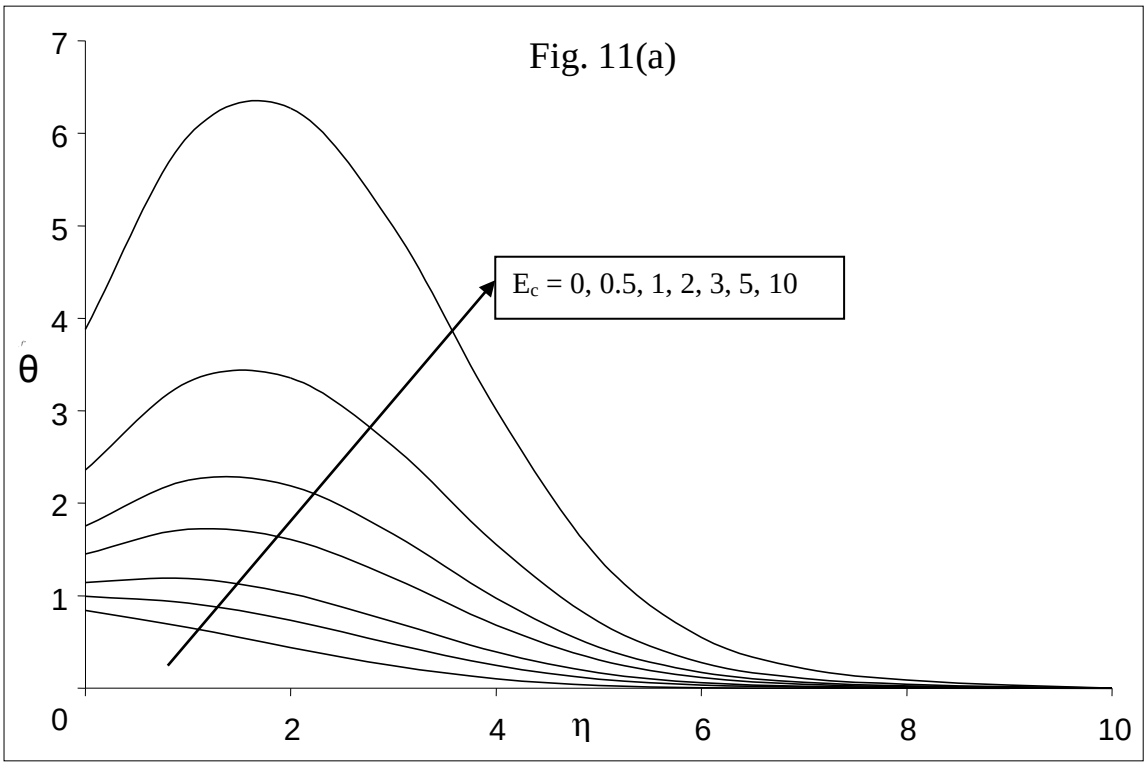

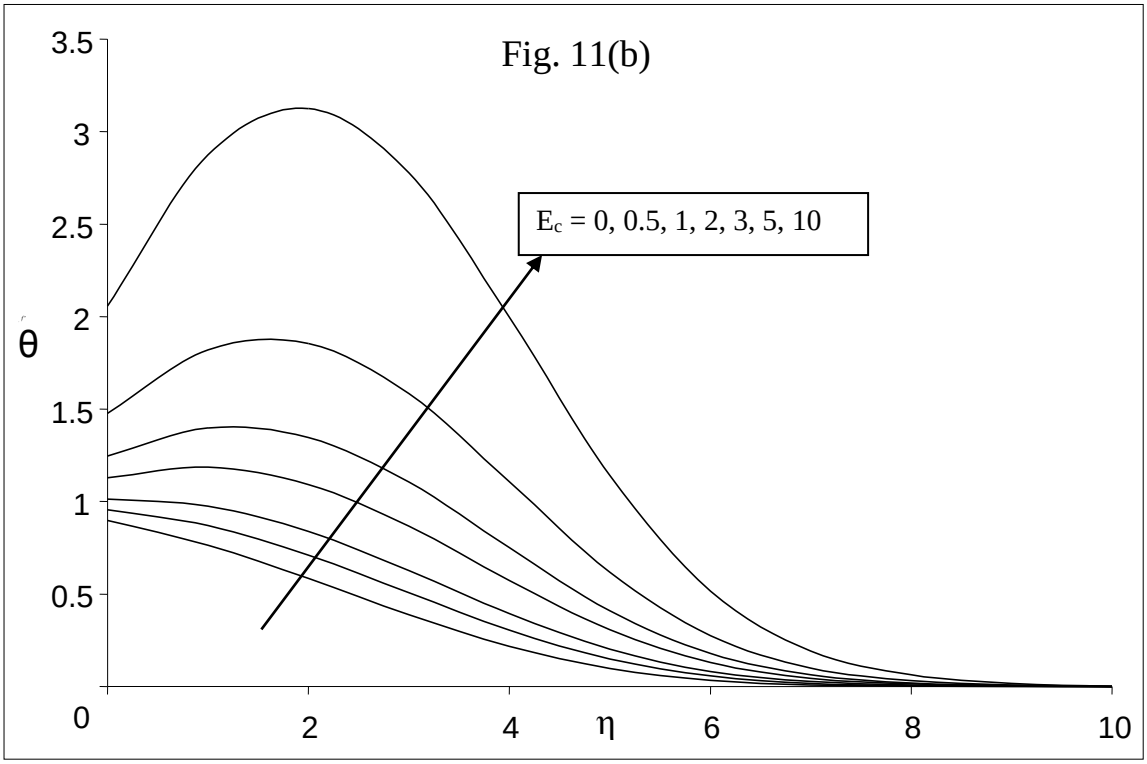

Fig. 11 Temperature profiles for various values of Eckert number E_c with $Kn_x = 1$, $\phi = 1$, $P_r = 0.72$, $R_d = 0$ and $M = 0.1$ **(a)** n = 0.5 **(b)** n = 1.0

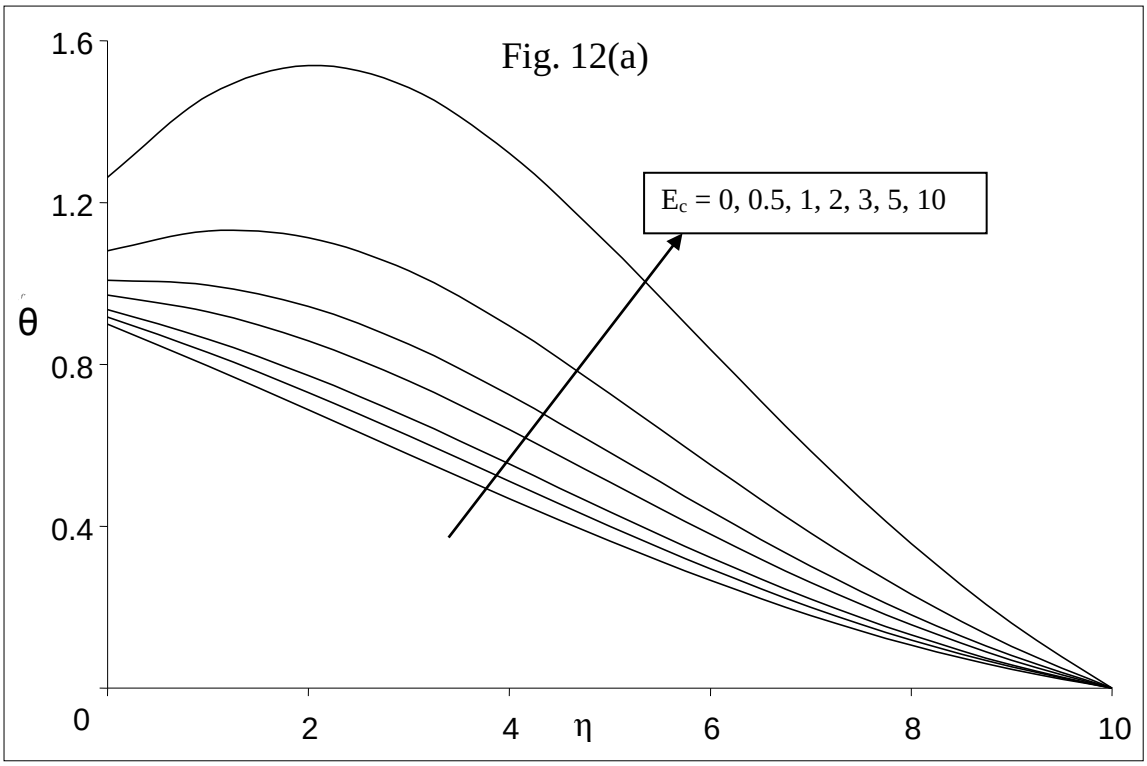

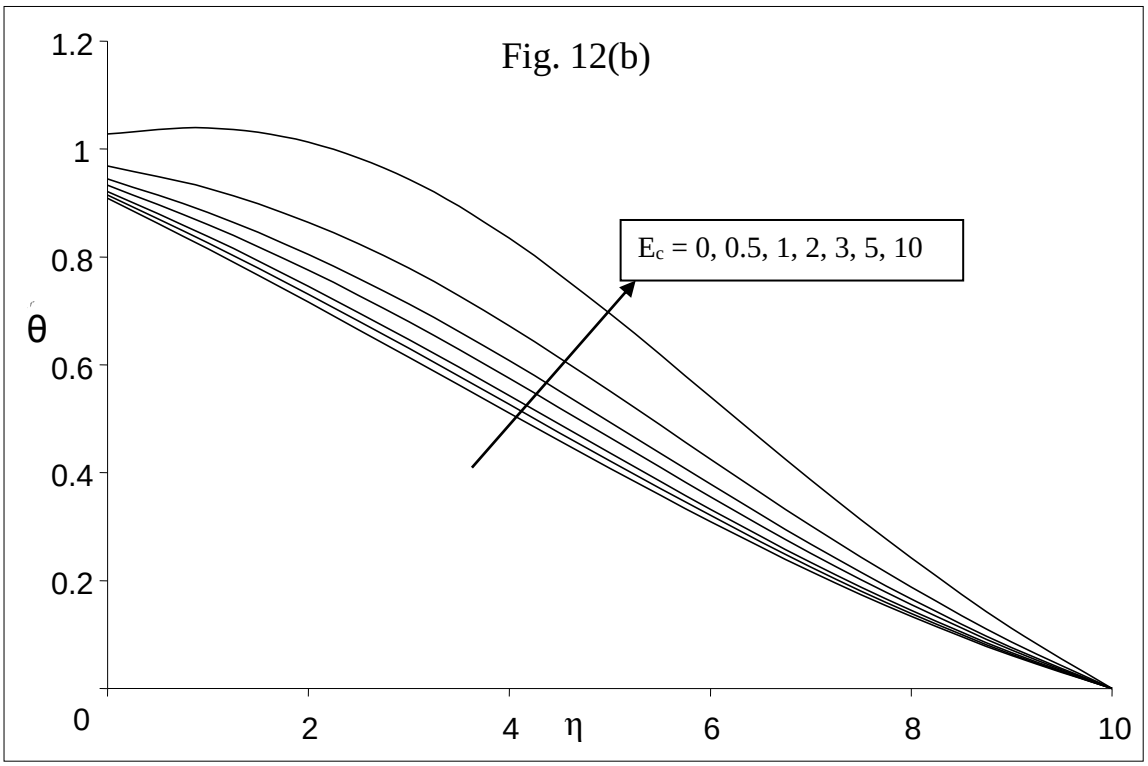

Fig. 12 Temperature profiles for various values of Eckert number E_c with $Kn_x = 1$, $\phi = 1$, $P_r = 0.72$, $R_d = 10$ and $M = 0.1$ **(a)** n = 0.5 **(b)** n = 1.0

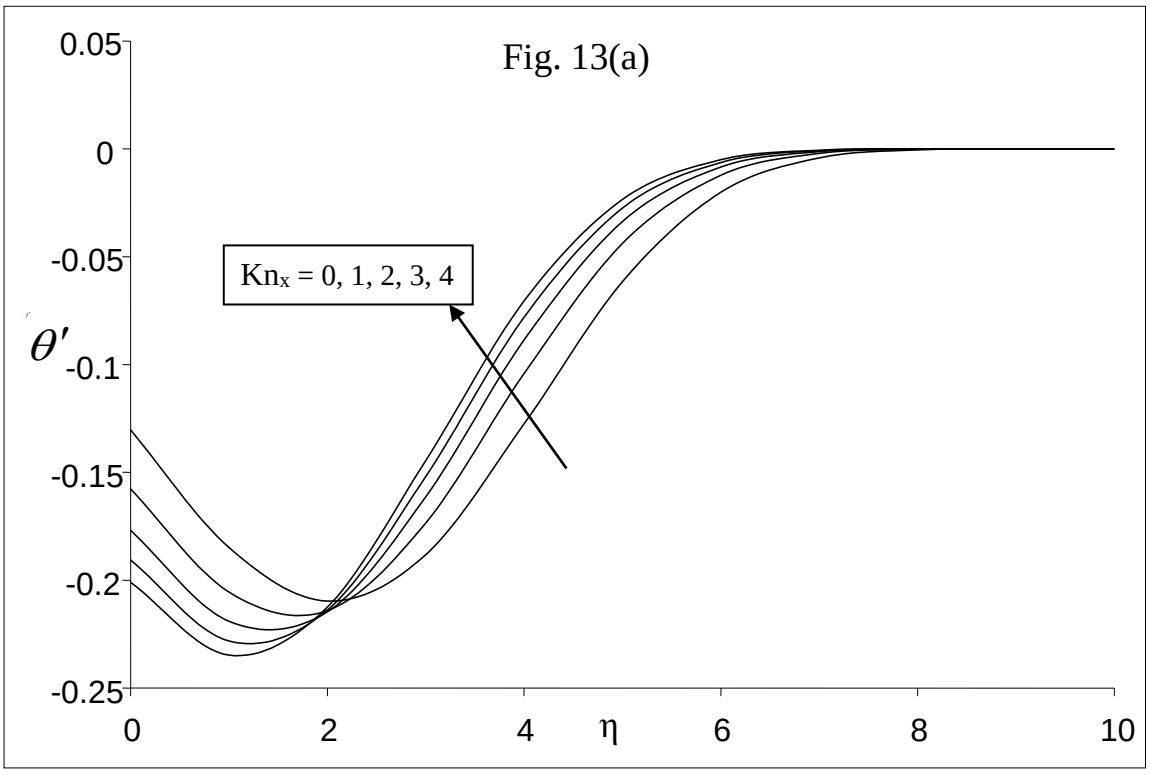

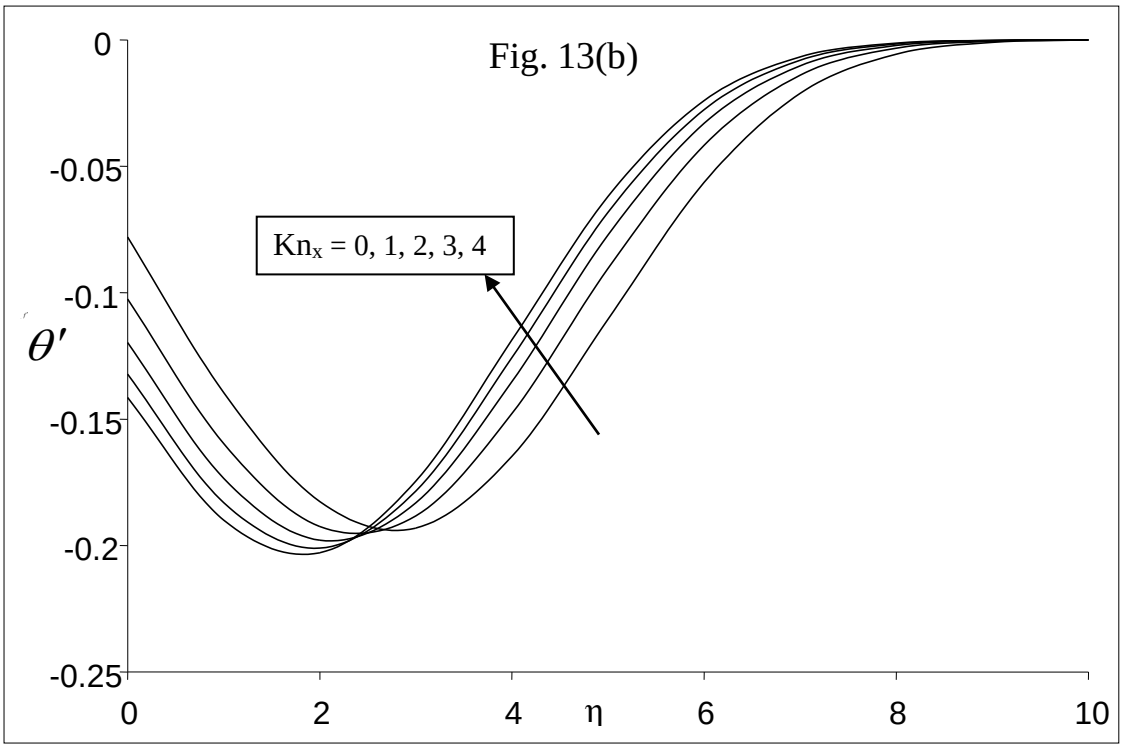

Fig. 13 Temperature profiles $\theta'(\eta)$ for various values of Knudsen number with ϕ = 1, P_r = 0.72, M = 0.1, R_d = 0 and E_c = 0 **(a)** n = 0.5 **(b)** n = 1.0

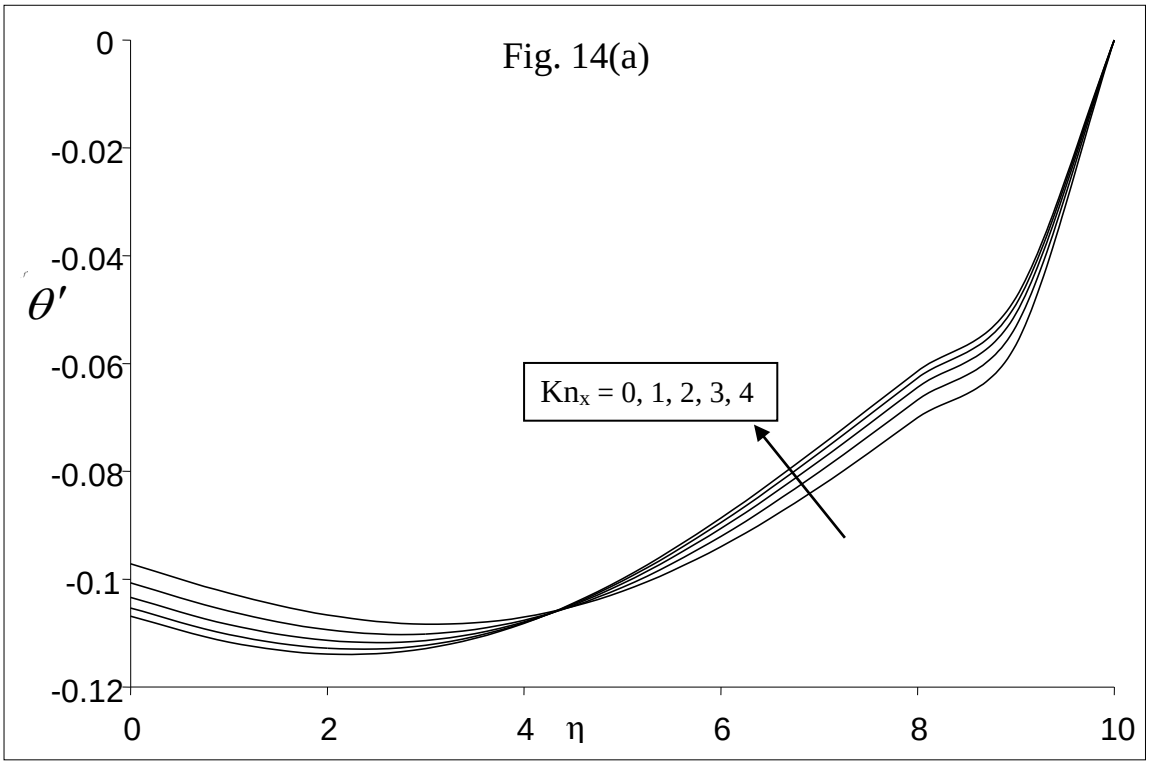

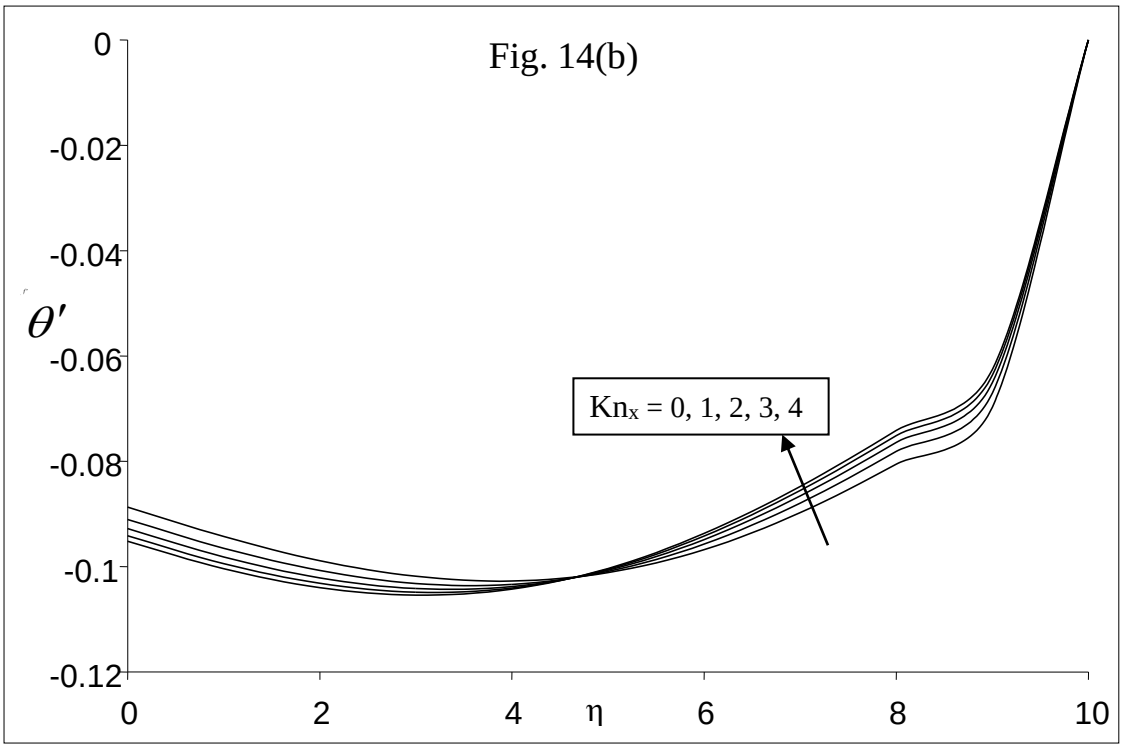

Fig. 14 Temperature profiles $\theta'(\eta)$ for various values of Knudsen number Kn_x with $\phi = 1$, $P_r = 0.72$, $M = 0.1$ $R_d = 10$ and $E_c = 0$ **(a)** n = 0.5 **(b)** n = 1.0

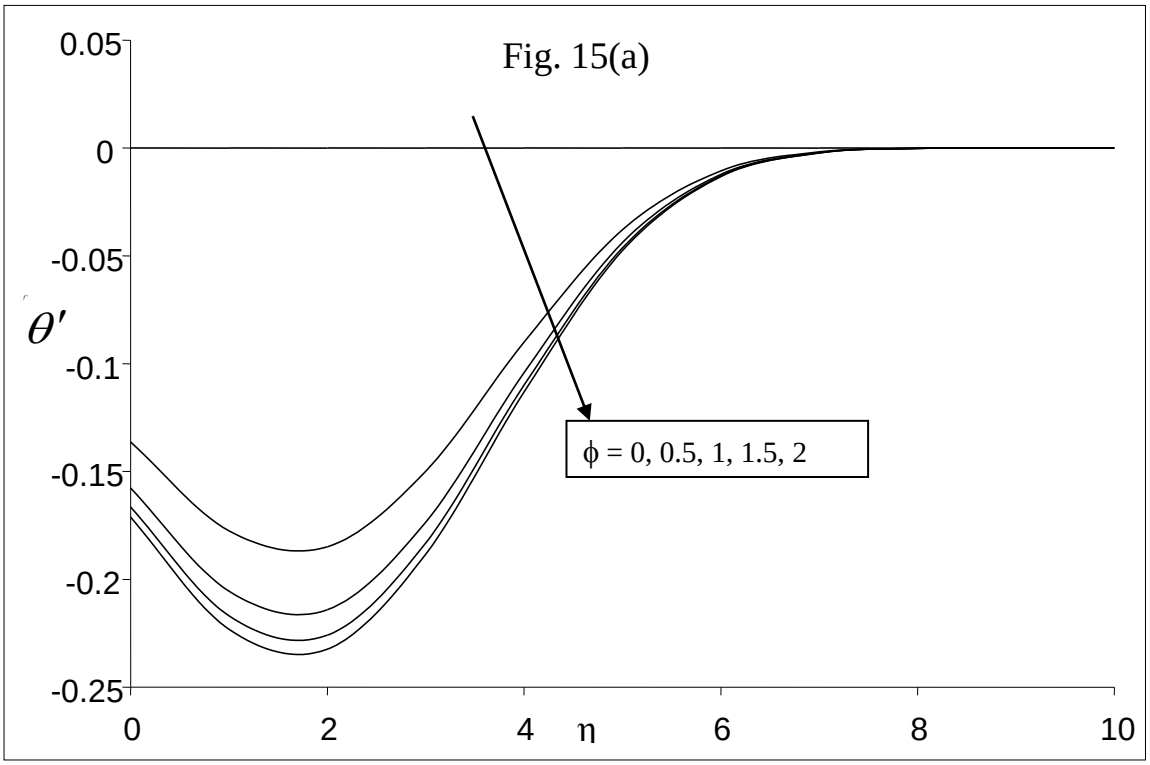

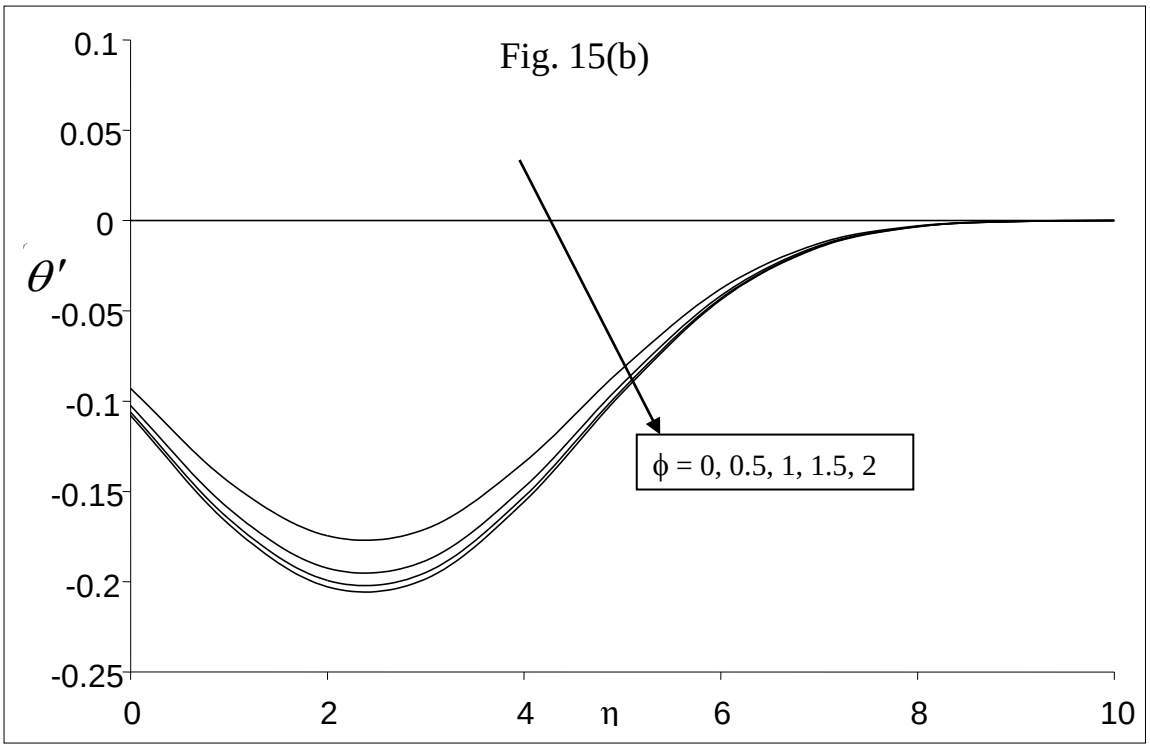

Fig. 15 Temperature profiles $\theta'(\eta)$ for various values of heat transfer coefficient φ with $Kn_x = 1$, $P_r = 0.72$, $M = 0.1$, $R_d = 0$ and $E_c = 0$ **(a)** n = 0.5 **(b)** n = 1.0

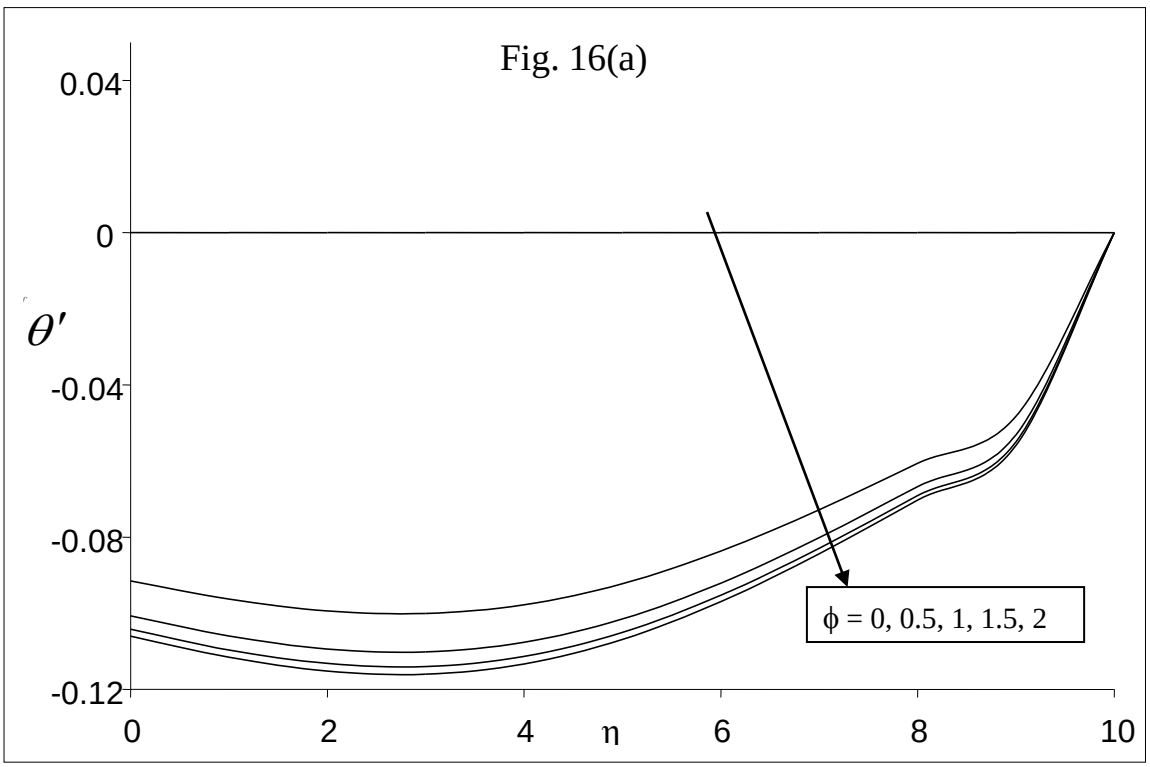

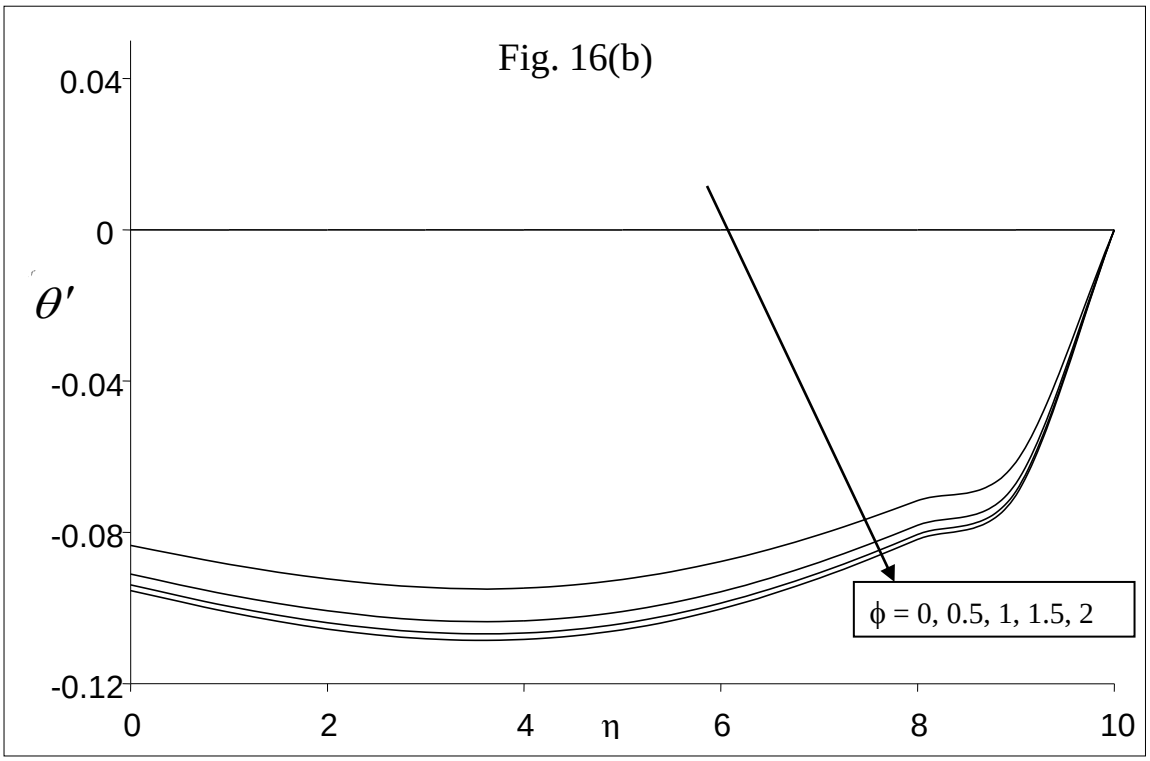

Fig. 16 Temperature profiles $\theta'(\eta)$ for various values of heat transfer coefficient φ with $Kn_x = 1$, $P_r = 0.72$, M = 0.1, $R_d = 10$ and $E_c = 0$ **(a)** n = 0.5 **(b)** n = 1.0

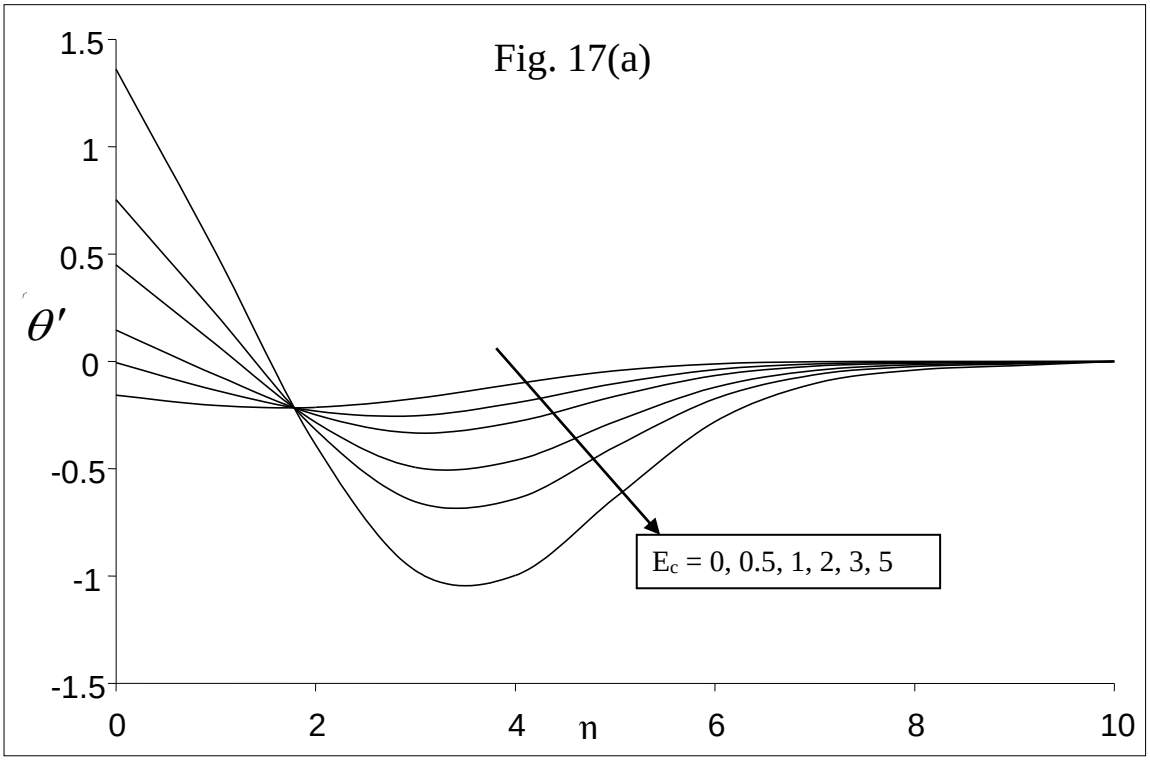

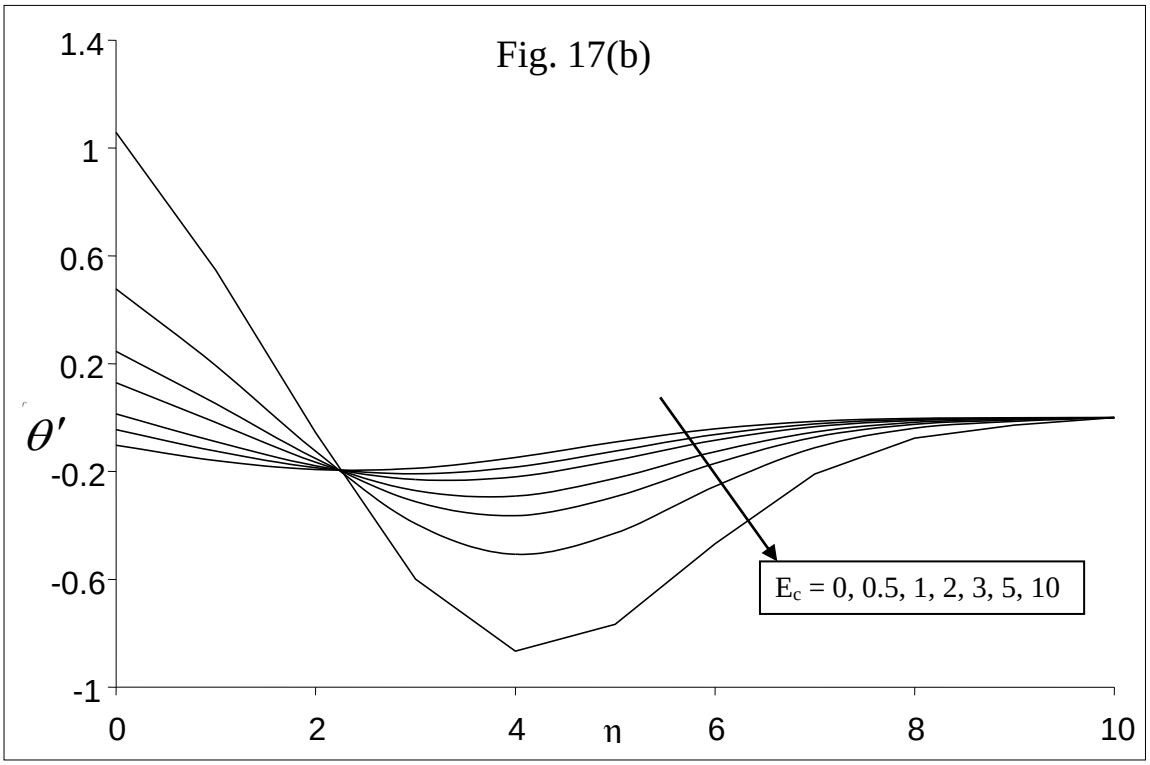

Fig. 17 Temperature profiles $\theta'(\eta)$ for various values Eckert number E_c with ϕ =1, Kn_x=1, M = 0.1, R_d = 0 and P_r = 0.72 **(a)** n = 0.5 **(b)** n = 1.0

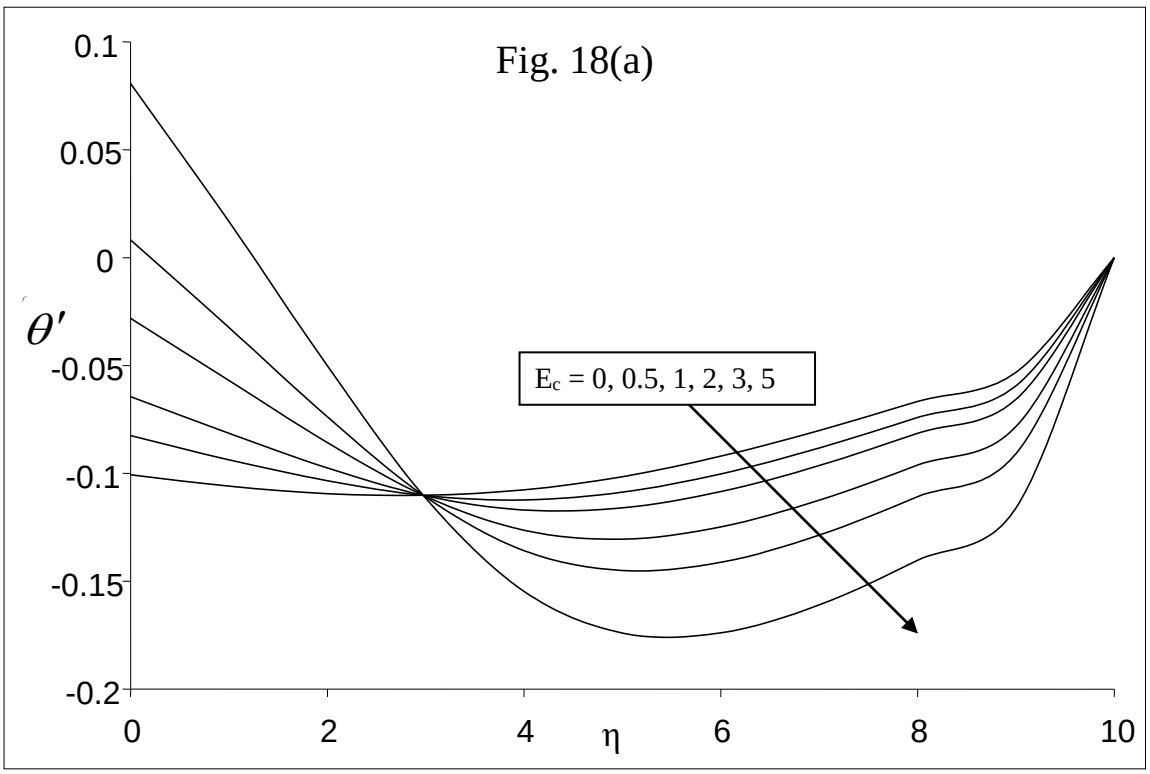

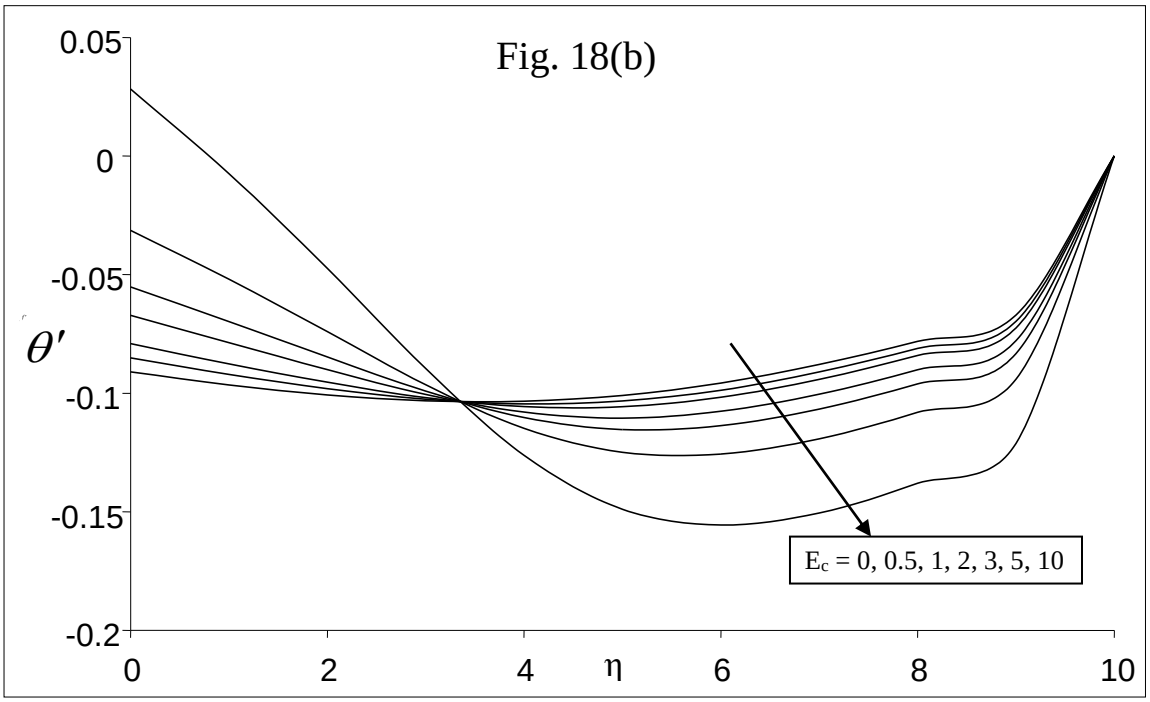

Fig. 18 Temperature profiles $\theta'(\eta)$ for various values Eckert number E_c with $\phi = 1$, $Kn_x = 1$, M = 0.1, $R_d = 10$ and $P_r = 0.72$ **(a)** n = 0.5 **(b)** n = 1.0

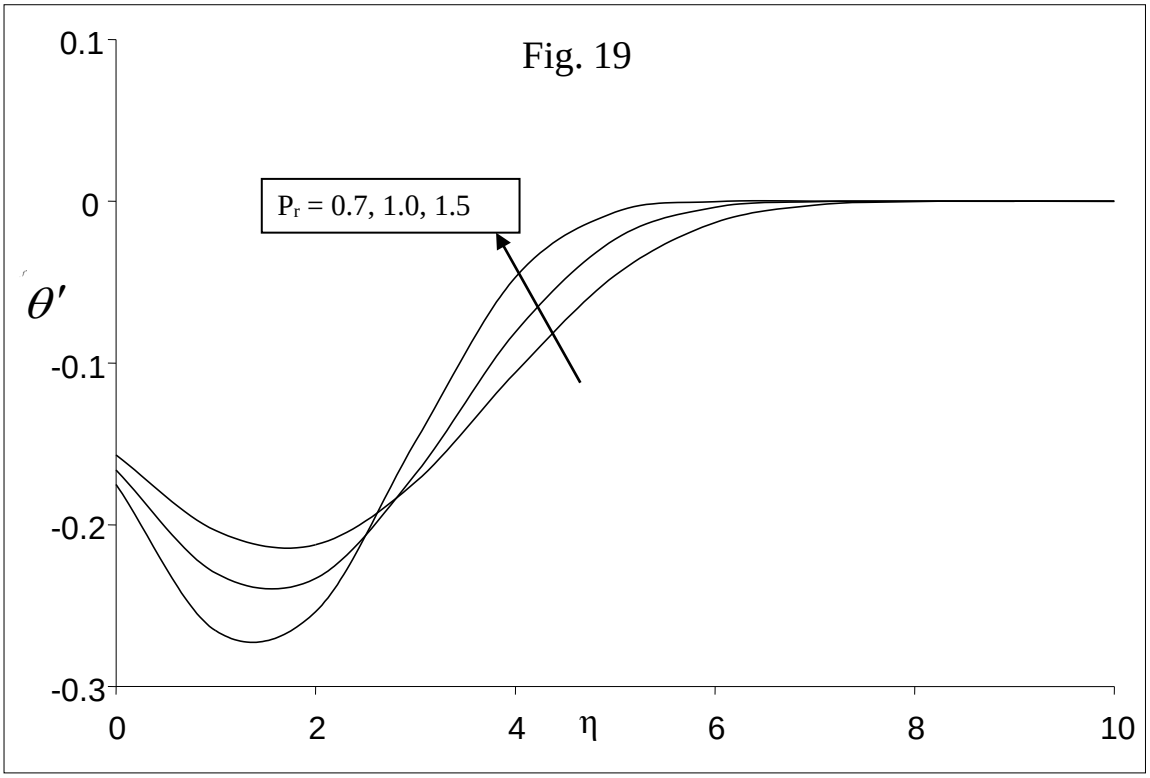

Fig. 19 Temperature profiles $\theta'(\eta)$ of pseudo plastic fluid for various values Prandtl number with $\phi = 1$, $Kn_x = 1$, M = 0.1, $R_d = 0$ and Ec = 0.0

REFERENCES

[1] Sakiadis, B. C., 1961, "Boundary layer behavior on continuous surfaces: Boundary layer equations for two dimensional and axisymmetric flow", A.I.Ch.E. J., 7, pp. 26-28.

[2] Nield, D. A., 2009, "The Beavers Joseph boundary condition and related matters: A historical and critical Note", Transp. Porous Med., 78, pp. 537-540.

[3] Cheng, C. Y., 2006, "Natural convection heat and mass transfer on non-Newtonian power-law fluids with yield stress in porous media from a vertical plate with variable wall heat and mass fluxes", International Journal in Heat and Mass transfer, 33, pp. 1156-1164.

[4] Neild, D. A., and Kuznetsov, A. V., 2003, "Boundary layer analysis of forced convection with a plate and porous substrate", Acta Mechanica, 166, pp. 141-148.

[5] Aziz, A. A., 2009, "Similarity solution for laminar thermal boundary layer over a flat plate with a convective surface boundary condition" Commun. Nonlinear Sci. Numer. Simulat., 14, pp.1064-1068.

[6] Cortell, R. B., 2008, "Radiation effect in the Blasius flow", Applied Mathematics and Computation, 198, pp. 333-338.

[7] Sarpkaya, T., 1961, "Flow of non-Newtonian fluids in a magnetic field", A.I.Ch.E.J., 7, pp. 324-328.

[8] Kumari, M., and Nath, G., 2001, "MHD boundary layer flow of a non-Newtonian fluid over a continuously moving surface with parallel free stream", Acta Mech., 146, pp. 139-150.

[9] Abo-Eldahab, E. M., and Salem, A. M., 2004, "Hall effect on MHD free convection flow of a non-Newtonian power-law fluid at a stretching surface", Int. Commun. Heat Mass Transfer, 2004, 31, pp. 343-354.

[10] Cheng, C. Y., 2006, "Natural convection heat and mass transfer of non-Newtonian power-law fluids with yield stress in porous media from a vertical plate with variable wall heat and mass fluxes", International Journal in Heat and Mass transfer, 33, pp. 1156-1164

[11] Guedda, M., and Hammouch, Z., 2008, "Similarity flow solutions of a non-Newtonian power-law fluid", Int. J. Nonlinear Sci., 6(3), pp. 255-264.

[12] Olajuwon, B. I., 2009, "Flow and natural convection heat transfer in a power-law fluid past a vertical plate with heat generation", Int. J. Nonlinear Sci., 7(1), pp. 50-56.

[13] Kishan, N., and Shashidar Reddy B., 2011, "Quasi linear approach to MHD effects on boundary layer flowe of power-law fluids past semi infinite flat plate with thermal dispersion", International journal of non linear science, 11(3), pp. 301-311.

[14] Ajadi, S. O., Adegoke, A., and Aziz, A., 2009, "Slip Boundary layer flow of non-Newtonian fluid over a flat plate with convective thermal boundary condition", Int. J. Nonlinear Sci., 8(3), pp. 300-306.

[15] Bellman, R. E., and Kalaba, R. E., 1965, "Quasi-Linearization and Non-linear boundary value problems", New York, Elsevier, 1965.